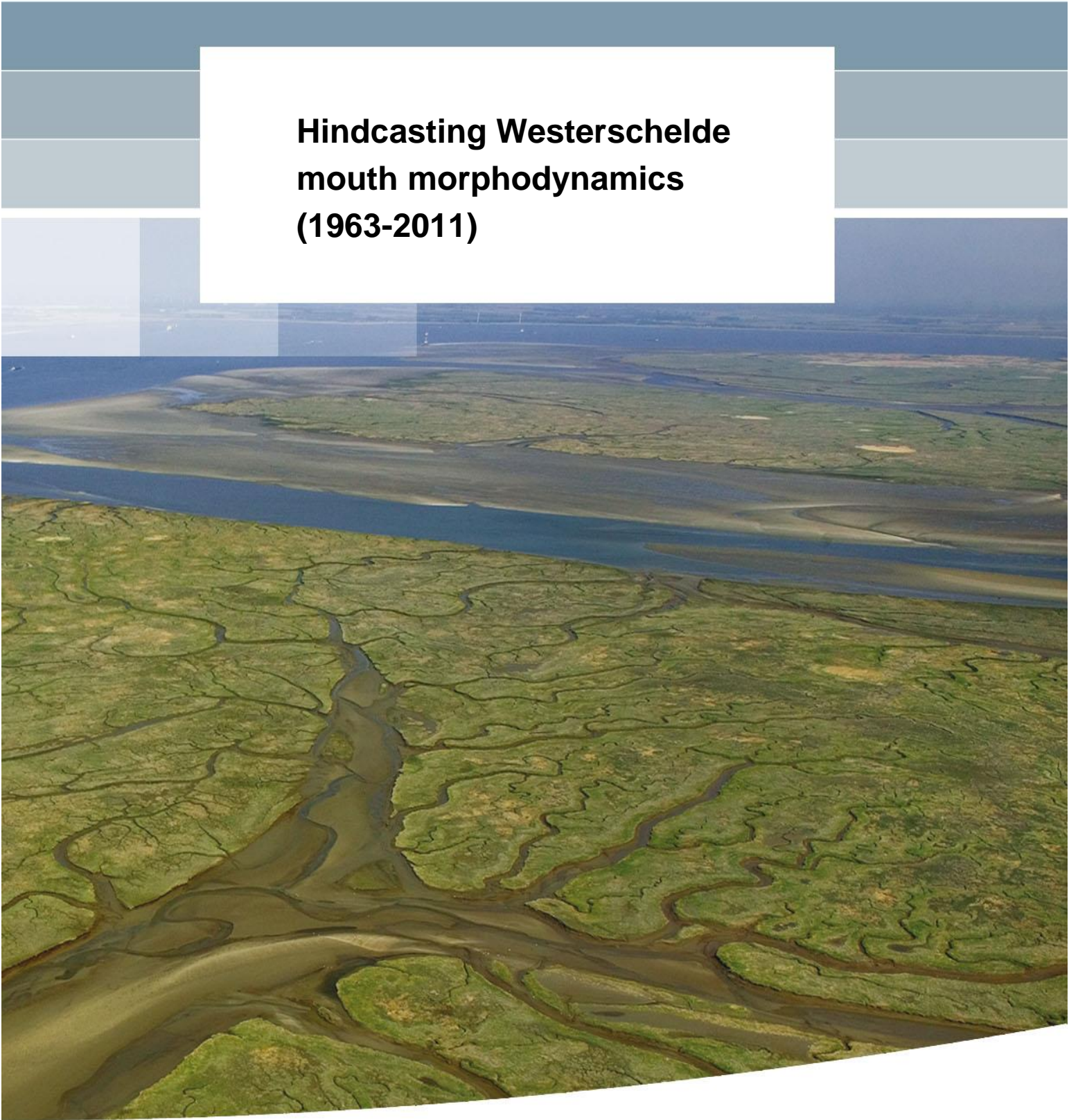


**Hindcasting Westerschelde
mouth morphodynamics
(1963-2011)**



Hindcasting Westerschelde mouth morphodynamics (1963-2011)

M. van der Wegen PhD
J.J. van der Werf MSc
P.L.M. de Vet
dr. B.R. Röpke

1210301-001

Title

Hindcasting Westerschelde mouth morphodynamics (1963-2011)

Project	Reference	Pages
1210301-001	1210301-001-ZKS-0006	32

Keywords

Long term morphodynamics, Westerschelde, Skill score

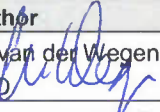



Summary

Within the framework of the Agenda for the Future defined by the Flanders-Dutch Scheldt Committee (VNSC), the Flanders Ministry of Public Works, department of Maritime Access (MOW-aMT) requested Deltares to carry out morphological research on the Westerschelde Mouth together with Waterbouwkundig Laboratorium Borgerhout (WL). In particular, this research concerns a Delft3D hindcast of the morphological developments of the Westerschelde mouth over the 1963-2011 period. This study thus provides an overview of how process-based modeling efforts can contribute to predicting decadal time scale morphodynamic developments.

The Delft3D model is based on the 2D NeVla model earlier developed and includes a schematised wind wave climate and dredging activities. Further sensitivity analysis concerns 3D and 2 sediment fractions. Long run times (about 10 days for 2D and 70 days for 3D) limited extensive sensitivity analysis.

Overall, modelled erosion and sedimentation patterns reflect main developments in the mouth over the 1963-2011 period. Model performance is better in the (more confined) Westerschelde itself, on longer time scales and in 3D with two sand fractions compared to 2D with a single sand fraction. Sensitivity runs excluding waves or dredging activities lead to less performance and indicate where waves or dredging activities have a large impact. In general, dredging activities have a larger impact than wave action. Although model results differ from observations, model skill becomes better over time. The model reaches positive Brier skill scores after 50 years but only in the confined inner parts. A possible reason is that the mouth morphodynamics is governed by more complex processes (e.g. wave action and sediment composition) that requires more subtle process schematization.

Future studies may forecast developments beyond 2011. These predictions can be carried out including interventions such as the dredging of the Geul van de Walvisstaart into an access channel. A process-based modelling effort assessing the impact of such an intervention would be more convincing when the intervention measures are large compared to the autonomous development of the system. Starting from a hindcasted bathymetry or starting from a measured bathymetry would in such as case be of limited importance

Version	Date	Author	Initials	Review	Initials	Approval	Initials
	jan. 2017	M. van der Wegen PhD		prof. dr. ir. Z.B. Wang		F.M.J. Hoozemans MSc	
		J.J. van der Werf MSc					
		P.L.M. de Vet					
		dr. B.R. R�bke					

State
final

Contents

1 Introduction	1
1.1 Framework	1
1.2 Background information	1
1.3 Aim	2
1.4 Relation to other models	2
2 Physical system and processes	5
2.1 Description of morphology and observed morphodynamics	5
2.2 Relevant processes	5
2.3 Sediments	6
3 Model setup	9
3.1 Requirements	9
3.2 Computational grids	9
3.3 Boundary and initial conditions	10
3.3.1 Hydrodynamic forcing	10
3.3.2 Initial bed level and sediment availability	10
3.3.3 Dredging and dumping	10
3.3.4 Other model settings and scenario overview	12
4 Results	15
4.1 Hydrodynamic validation	15
4.2 Trends in bathymetric development	16
4.3 Erosion and sedimentation patterns	18
4.4 Skill scores	21
4.5 Sediment availability	25
4.6 Dredging and dumping volumes	25
5 Discussion and conclusions	27
6 Future work	29
7 References	31
Appendices	
A Derivation of wind wave climate	A-1
A.1 Introduction	A-1
A.2 Available data	A-1
A.2.1 Overview	A-1
A.2.2 Wave data	A-2
A.2.3 Wind data	A-3
A.3 Wave climate schematization	A-4
A.3.1 Morphological tide	A-5
A.3.2 Derivation of wave conditions	A-5
A.3.3 Validation of wave schematizations	A-10

A.4	References	A-15
B	BSS definition	B-1
C	Detailed model results	C-1
D	Detailed model results of dredging activities	D-1

1 Introduction

1.1 Framework

The Netherlands and Flanders work together on the policy-making and management of the Westerschelde estuary in the Flanders-Dutch Scheldt Committee (VNSC). The Agenda for the Future (AvdT) defines the joint research efforts for the 2014-2017 period.

Within the framework of the AvdT, the Flanders Ministry of Public Works, department of Maritime Access (MOW-aMT) has requested Deltares to carry out morphological research on the Westerschelde Mouth together with Waterbouwkundig Laboratorium Borgerhout (WL). In particular, this research concerns the development and application of a morphological, numerical modelling toolset considering explorations on the future state of the Scheldt estuary.

Within this framework, the “Vlaamse Baaien” project explores the feasibility and possible impact of large scale morphological interventions at the mouth of the Westerschelde (Western Scheldt) to secure sustainable development of the region. Within this project there was a need identified to assess the morphological impact of significant adaptations in the Westerschelde mouth.

A first step towards such an assessment would be to explore the skill of Delft3D in hindcasting observed, decadal timescale, morphological developments. A subsequent step is then to forecast developments with and without intervention measures. The intervention measures include the extension of the Port of Zeebrugge and associated dredging works as well as dredging works carried out within the Westerschelde to safeguard access to the Port of Antwerp.

The Delft3D modelling suite is highly suitable as it provides a flexible tool to assess morphodynamic developments allowing for quick adaptations of the model setup and inclusion or exclusion of various processes.

1.2 Background information

Autonomous (i.e. without anthropogenic interference) morphodynamic development in estuaries and adjacent coasts takes typically place at long, decadal timescales. In contrast, port development works like breakwater construction and access channel dredging have an immediate and local impact on morphodynamic developments, but they may also influence the estuarine morphodynamics at larger time and spatial scales. For sustainable port development, it is important to assess future morphodynamic developments and to estimate the costs of related dredging operations.

The Port of Zeebrugge is an example of a port that has a large impact on the local morphology by its breakwaters, while regular maintenance dredging of its access channel is required. In addition, its access channel is part of a larger access channel leading to the ports of Vlissingen in the Westerschelde and Antwerp along the Scheldt River.

Elias and Van de Spek (2015) provide a comprehensive overview of observed bed level dynamics at the Westerschelde Mouth over past decades (Figure 1.1 and Figure 1.2). The migration and evolution of channels and shoals are attributed to breakwater construction, dredging and deposition of dredged material, as well as the autonomous evolution of the

system (i.e. evolution not directly imposed by human interference). An important question is whether or not process-based models like Delft3D and Finel are able to reproduce these observed dynamics.

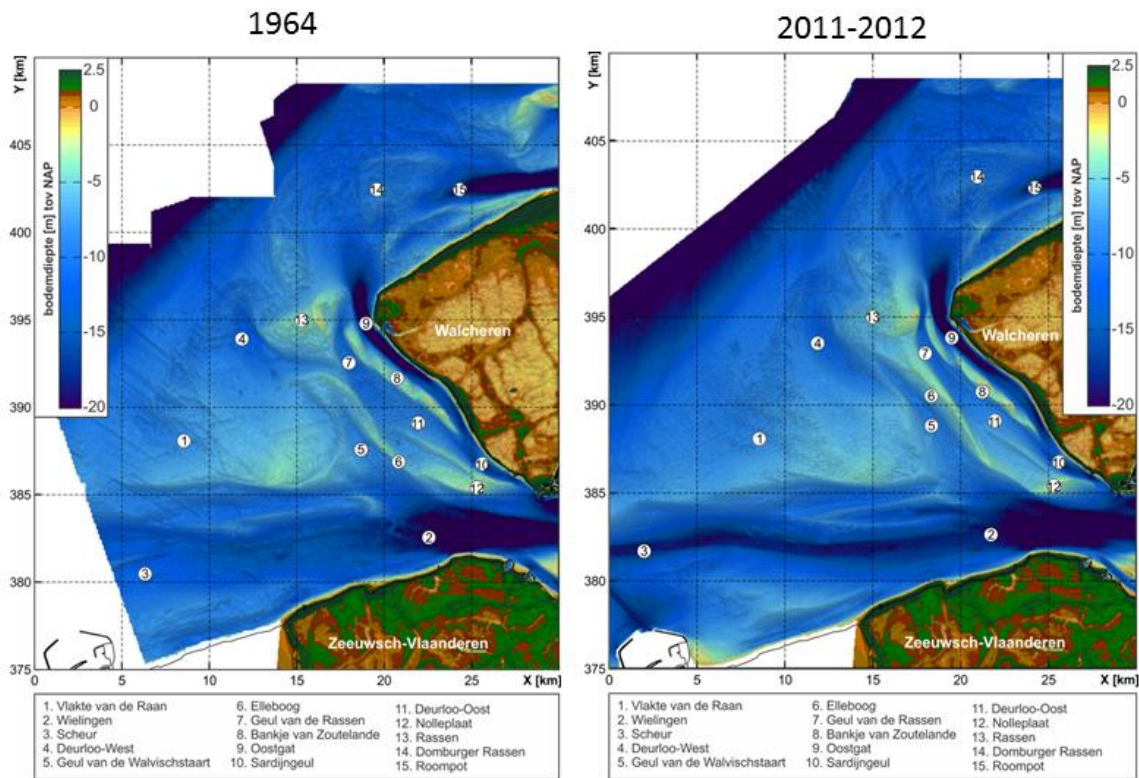


Figure 1.1 Overview of channels and shoals in the Westerschelde Mouth. The bathymetry is based on the 1964 and 2010–2011 measurements (from Elias and Van der Spek (2015)).

1.3 Aim

The aim of this study is to assess the skill of Delft3D in hindcasting morphological developments between 1963 and 2011 covering the entire Westerschelde but with an emphasis on its mouth. This study will form the basis of other studies in which different future scenarios of access channel dredging will be considered.

1.4 Relation to other models

In an attempt to hindcast measured morphodynamic development in the Westerschelde between 1860 and 1970 with a model similar to Delft3D (Finel), Dam et al. (2013, 2016) demonstrate a significant model skill (BSS = 0.5) after 110 years (Figure 1.3 and Figure 1.4). An important observation is that the skill of the model is quite weak (even negative) in the first decades but significantly increases over time. Dam et al. (2013, 2016) attribute this to the importance of the Westerschelde plan form which has an initially small but continuously growing impact on the morphodynamic development. The weak initial skill score is attributed to the fact that process descriptions and initial and forcing conditions are limited. For example, waves and storm impact are not accounted for and some process formulations are quite rudimentary or not included at all (i.e. bed slope effect and sediment distribution). As a result the associated relative error is large at the start of the hindcast but decreases on the longer term when the geometrical influence becomes more pronounced. An important remaining question is whether or not process-based models will lead to similar skill scores in less bounded and more wave influenced areas, such as the mouth of the Westerschelde.

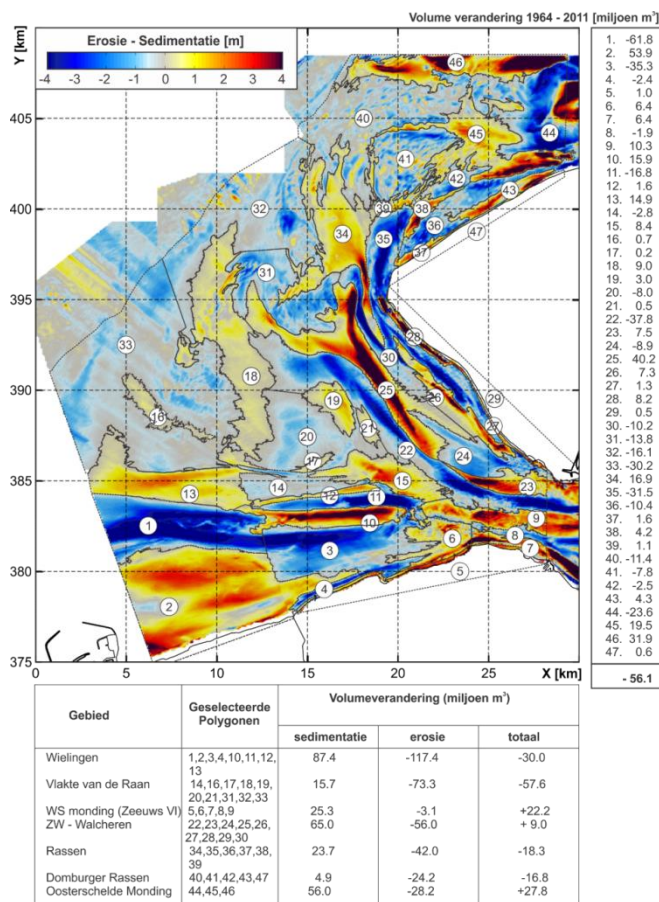


Figure 1.2 Cumulative erosion and sedimentation observed in the Westerschelde mouth between 1964 and 2011 and partial volume balances for the 1964-2011 period (from Elias and Van der Spek (2015)).

For past hydrodynamic and morphodynamic studies, the NeVla model (see for earlier applications Vroom et al 2015b, Van der Werf et al, 2013) has been developed covering the entire Westerschelde. The current study applies the NeVla model in 2D, considering only sandy sediments and including wind waves and dredging operations. Thus, the model is able to address the impact of morphological interventions at the Westerschelde mouth on tidal amplitude fluctuations in Antwerp on a decadal time scale. This is an important feature since tidal amplitude amplification within the Westerschelde (possibly as the consequence of interventions at the mouth) may have serious consequences for flooding frequency (high water) and port access (low water).

Within the larger framework of the current study, the ZWEM model is more detailed than the NeVla model, being 3D and including sand and mud fractions to describe fine sediment deposition patterns observed in the Port of Zeebrugge access channel. To limit computational time the model domain only extends landward till Ossensisse midway the Westerschelde and periods covered about 1 year only. In addition and on the other side of the time period spectrum, the Waterbouwkundig Laboratorium has been working on a more schematised Delft3D modelling approach covering centuries of morphodynamic developments and exploring the long-term impact of possible human interventions.

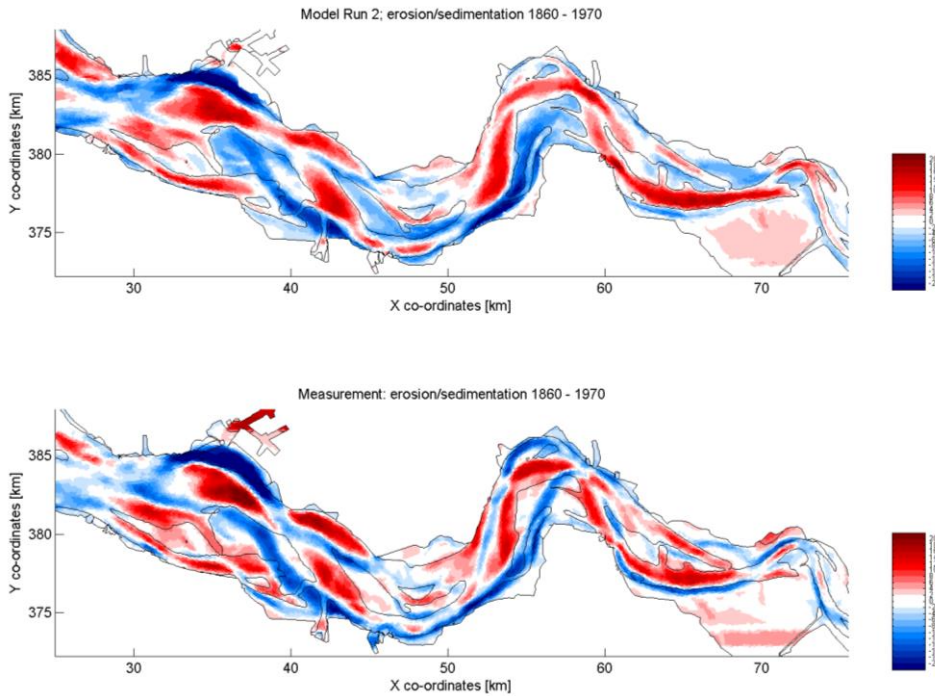


Figure 1.3 (a) Modelled and (b) measured cumulative erosion and sedimentation patterns in the Westerschelde between 1860 and 1970 (from Dam et al., 2013).

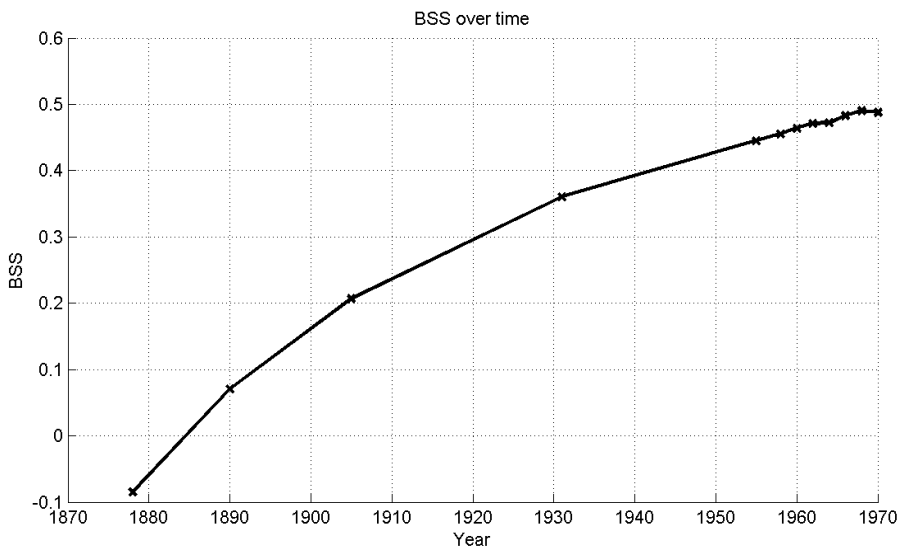


Figure 1.4 Brier Skill Score over time of the domain covered in figure 1.4 (from Dam et al., 2013).

2 Physical system and processes

2.1 Description of morphology and observed morphodynamics

The Westerschelde mouth is roughly located between the seaward -20 MSL contour line, parallel to the shoreline of Belgium and Zeeland and the relatively narrow entrance to the Westerschelde around the line Vlissingen-Breskens. A major feature is the triangular shaped shoal, Vlake van de Raan, with depths ranging from MSL -2.5m to -10m. The Westerschelde mouth is intersected by two main channels, viz. the Wielingen and the Oostgat, of which the Wielingen is by far the largest. About a century ago there was a shift from a three-channel system towards the current two-channel system. The two-channel system has been relatively stable despite the partly closure of the Eastern Scheldt in 1985 and several dredging operations to enlarge the depth of the access channel towards the port of Antwerp in the Westerschelde itself (Van der Slikke (1997), Van Enckevoort (1996), Cleveringa (2006) and Cleveringa (2008)).

Regular dredging activities have been securing access to the Port of Zeebrugge (in the Geul and Pas van Zand) and the Port of Antwerp (in the Wielingen and the Westerschelde itself). For example, between 1964 and 2011 a clear signal of dredging activities can be observed by the deepening of the Wielingen (Figure 1.1). Furthermore, Zeebrugge Port expanded between 1972 and 1985 by enlarging its breakwaters.

The morphology of channels at the northern part of the mouth is more complex and less directly affected by dredging activities. In seaward direction, the Sardijngeul splits into the Oostgat aligned directly along the shore and, located more westerly, Deurloo-Oost merging with the Geul van de Rassen. Even more westerly, the Geul van de Walvisstraat aligns with Deurloo-West in an ebb-flood channel configuration in 2011. Between 1964 and 2011 the connection between Geul van de Rassen and Deurloo-West faded while Deurloo-West and Geul van de Walvisstraat almost merged. The Rassen shoal moved more into the mouth connecting the Elleboog shoal, while squeezing the Geul van de Rassen and the Oostgat.

Based on historic data analysed by Van Enckevoort (1996), Van Oyen et al. (2016) describe changes of the Westerschelde mouth covering the period 1800-1978. An important aspect of this study is the description of the Deurloo channel that existed between Oostgat and Wielingen between 1823-1932. Based on an analysis of more recent bathymetries measured almost at yearly intervals in the 1963-2011 period, Elias and Van der Spek (2015) describe the morphological developments in more detail. The main erosion and sedimentation patterns as the results of the trends in autonomous morphological developments and dredging activities could be described between 1964 and 2011 (Figure 1.2). However, it was difficult to derive a trustworthy year-to-year sediment budget since measurements accuracies were of the same order as observed morphological developments (Cleveringa (2008), Elias and Van der Spek (2013)).

2.2 Relevant processes

Hydrodynamic processes (tides, wind waves, density driven currents and wind induced currents) drive sediment transports and steer morphological developments.

Tidal dynamics are probably the most important forcing of the Westerschelde mouth and determine the size, location and direction of the main channels. Based on a modelling study, Damen (2014) suggests that tidal currents are the main driver of the Oostgat erosion adjacent to the shoreline. Another example is the size, location and direction of the Wielingen, located

at the southern shoreline. The dominance of southern channels is apparent at inlets along a large part of the Dutch coast. An explanation is found in the observation that the phasing of ebb and flood is similar at the mouth and in the Westerschelde. Along shore directed flood flows at the foreshore occur simultaneously with flood flow entering the Westerschelde ((Van Veen (1936), Sha (1993), Dissanayake et al. (2009)). As a result, the Wielingen has been conveying the largest part of the incoming tide from the south into the Westerschelde and the outgoing tide towards the south, leading to channel expansion and the current large size and direction of the channel.

Various studies describe tide residual currents in the Westerschelde mouth resulting from tidal asymmetries (Steijn & Van der Spek, 2005; Van der Werf & Brière, 2013; Tonnon & van der Werf, 2014) which are partly confirmed by measured bed forms (Erkens, 2003). E.g. residual currents in Wielingen, Deurloo-Oost and the northern part of the Oostgat are ebb directed while they are flood directed in the southern part of the Oostgat and the Sardijneul.

The Westerschelde Mouth is exposed to wind wave action originating from the North Sea and the English Channel. Waves will increase shear stresses while propagating across shoals and breaking at shores. This leads to stirring up of sediments that are transported by tidal currents and, to a lesser extent, wave driven currents. The impact of waves will be most pronounced at shallow shoals possibly and eventually driving their migration. We are not aware of studies pointing to areas where wave action is governing the morphodynamics at the Westerschelde mouth.

Density driven flows are present due to the saline water at the North Sea and the fresh water discharge from the Scheldt River. The river flow is very small compared to the tidal volumes leading to weak gravitational circulation. Despite its weakness, this density flow still plays an assumed important cumulative role in landward transport of fine marine sediments in particular. Although studies exist on fine sediment dynamics in the Westerschelde (e.g. Van Kessel et al. (2011)), they have not been very conclusive on the impact of long-term residual (and density driven) fine sediment dynamics in the Westerschelde and its mouth. In addition, the impact of density driven flows on coarser sandy sediments has not been explored.

2.3 Sediments

Originating from the Calais cliffs and the Channel, there is a northward residual transport of fine sediment along the Belgian and Dutch coast. Associated suspended sediment concentrations are several 10's of mg/l while the extent of the turbid zone varies seasonally from 10 km (summer) to 20 km (winter) seaward from the coastline (Fettweis et al., 2003, 2007). A turbidity maximum prevails around the Port of Zeebrugge. This may originate from the supply of fine sediments from the Channel in combination with local tidal asymmetries (Fettweis et al., 2003, 2007), but also from a bathymetric Holocene source (a currently submerged, 3000 year old mudflat-marsh system, Lauwaert et al. (2006), Vroom et al 2016).

The following analysis puts yearly transport volumes around the Westerschelde mouth in a broader perspective. Fettweis et al. (2007) estimate the northward directed fine sediment transport along the French coast to be about 20 Mton/year in a 10-20 km wide stretch across the shore, corresponding to 7.5 Mm³/year based on a 2650 kg/m³ density. In contrast, sandy transports mainly occur in the surf zone close to the shore line and amount up to 0.4 Mm³/y along the Belgian coast south of Zeebrugge (Verwaest et al, 2011) and the Dutch coasts north of Hoek van Holland (Van Rijn, 1997). As a reference, the tide-residual sand transports through the cross-section Vlissingen-Breskens (as calculated by the model described in this

report) are about 1.2 Mm³/y, whereas the transport volume amplitudes during ebb or flood (not tide-residual) are typically an order of magnitude larger.

The largest part of the Westerschelde mouth consists of sandy sediments with grain size varying from 100 µm mainly at the shoals to 800 µm in the deeper portions of larger channels. In addition, non-erodible layers exist in the Westerschelde itself. These layers consist of Pleistocene layers, peat layers and highly consolidated clay and are maybe not non-erodible, but hard to erode. Nevertheless, these layers are considered non-erodible. Following Dam et al (2013) erodible layers were determined based on work by Gruijters et al. (2004). The level of the non-erodible layer and the actual measured bed level determine the height of the layer with erodible sediments. Van de Male (2004) and Dam (2012) determined where these layers were intersected by historically observed bathymetries (areas that have been covered with sand afterwards and thus should consist of erodible material). Figure 2.2 shows that, as the result of this methodology, large parts of the Westerschelde mouth were defined as non-erodible. However, Van der Spek (personal communication) suggests that large parts should be sandy and that the sediment thickness for the Westerschelde mouth in Figure 2.2 mainly result from low resolution coring and the fact that major shallow parts just have not been incised by channels historically.

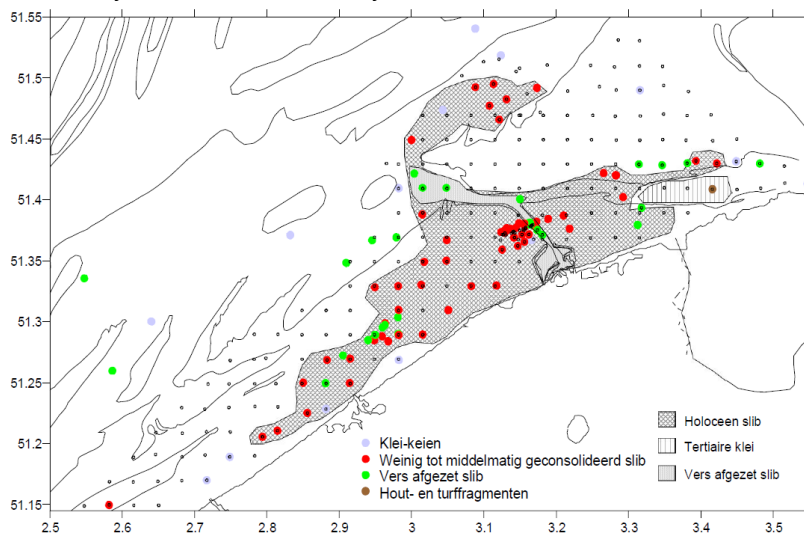


Figure 2.1 Distribution of cohesive sediments around port of Zeebrugge. Cores were taken at dots while black dots indicate sandy sediment, from Lauwaert et al. (2006).

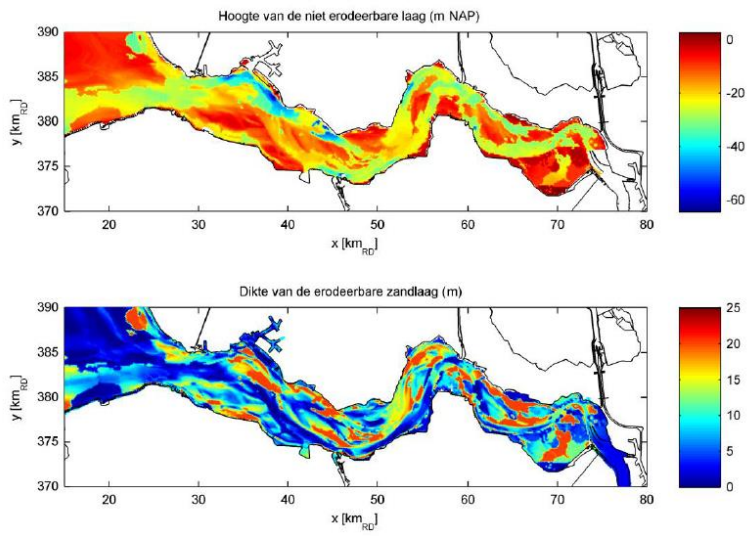


Figure 2.2 Height of the non-erodible layer wrt MSL (upper panel) and thickness of the erodible sand layer (from Dam et al 2013)

3 Model setup

3.1 Requirements

- The model domain should cover the entire Westerschelde to evaluate (in this and possible following studies) the impact of intervention measures at the mouth on the entire Westerschelde.
- Grid resolution should be small enough to cover main channels in the Westerschelde and its mouth.
- Run times should be acceptable (< 2 weeks on the Deltares cluster) to enable sensitivity analyses covering multidecadal periods (1963-1984 (up to the end of the Zeebrugge Port expansion), 1984-2011, 2011-2042 (forecast)).
- Waves should be included.

As a results of these requirements, we took the NeVla model as the basis for our model since this model was calibrated and validated before in several studies and meets all the requirements mentioned above.

3.2 Computational grids

The Delft3D model consists of a coupled flow and wave model. The flow model consists of 5 domains (Fig. 3.1) with a grid resolution of maximum 4 m in the Westerschelde tributaries and of minimum 500 m in the shelf. Assuming that wave penetration from the sea and local wave generation is not significant for landward domains and to save computational cost, the wave model only covers domains 1 and 2 where the grid was derefined by factor 2 compared to the flow grid.

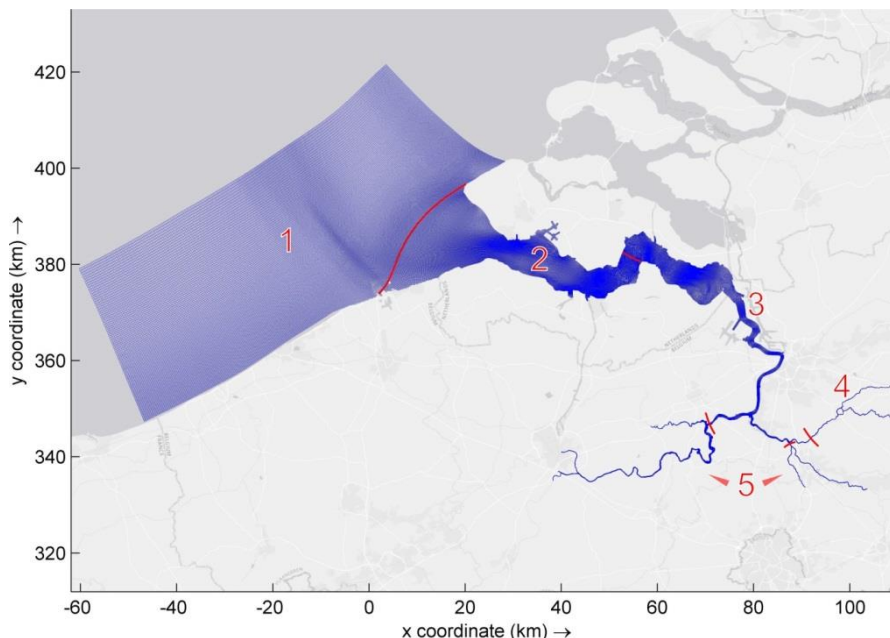


Figure 3.1 Schematic diagram showing the 5 domains of the NeVla flow model grid. The grid resolution ranges between maximum 4 m in the tributaries of the Westerschelde and minimum 500 m in the shelf.

3.3 Boundary and initial conditions

3.3.1 Hydrodynamic forcing

The hydrodynamic boundary conditions consist of a tide, river and wave component. Tides and river - In the flow model and following Van der Werf et al. (2013), 32 tidal constituents were considered, derived from the ZUNO model by nesting and bi-linear interpolation along the open boundaries of domain 1 of the NeVla model. The tidal constituents are thus based on analysis of the 2011 conditions. The tidal boundaries were based on the Riemann invariant in the north and the current boundary type in the west and the east. Along the western current boundary, an alpha reflection parameter of 400 was used in order to avoid unintended wave reflections. Fluvial forcing in the flow model is realised by discharge cells at the river boundaries using corresponding discharge measurements.

Waves - The boundary conditions of the wave model were taken from Van Rooijen et al. (2015), see Appendix, who schematised the prevailing, long-term wave climate into 1, 2, 4 and 6 wave conditions based on data from the Schouwenbank wave buoy.

3.3.2 Initial bed level and sediment availability

The initial bed level was derived from measured data of the year 1963. The available sediment (erodible sediment layer thickness) for the 1963 conditions was derived by adapting the erodible layer thickness belonging to the 2011 bathymetry applied by Van der Werf et al. (2013) into the 1963 bathymetry.

3.3.3 Dredging and dumping

Dredging and dumping activities in the main navigation channel of the Westerschelde were included following the overview by Vroom et al (2015a). This was realised by implementing corresponding dredging polygons each associated with a specific minimum water depth (Figs. 3.2 and 3.4). Material dredged here was then deposited in specified dumping areas (Figs. 3.3 and 3.5). As some of the dredging activities started later in the simulation period from 1964 to 2011, the time varying dredging functionality was used.

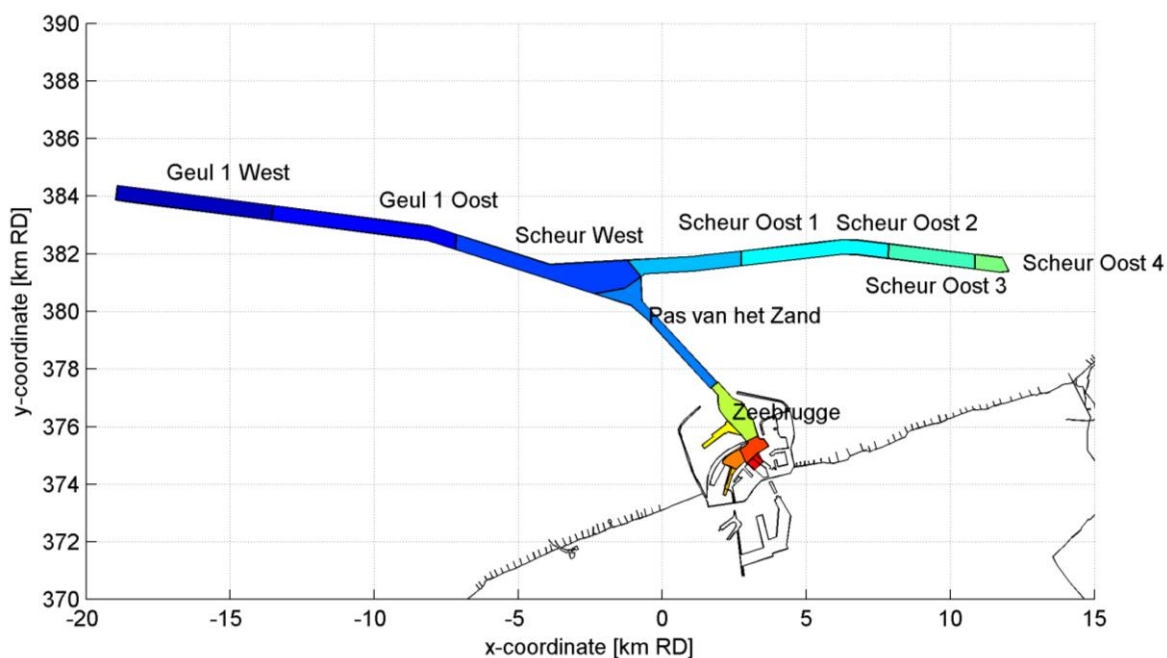


Figure 3.2 Location of dredging zones in the shelf area (from Vroom, 2016)

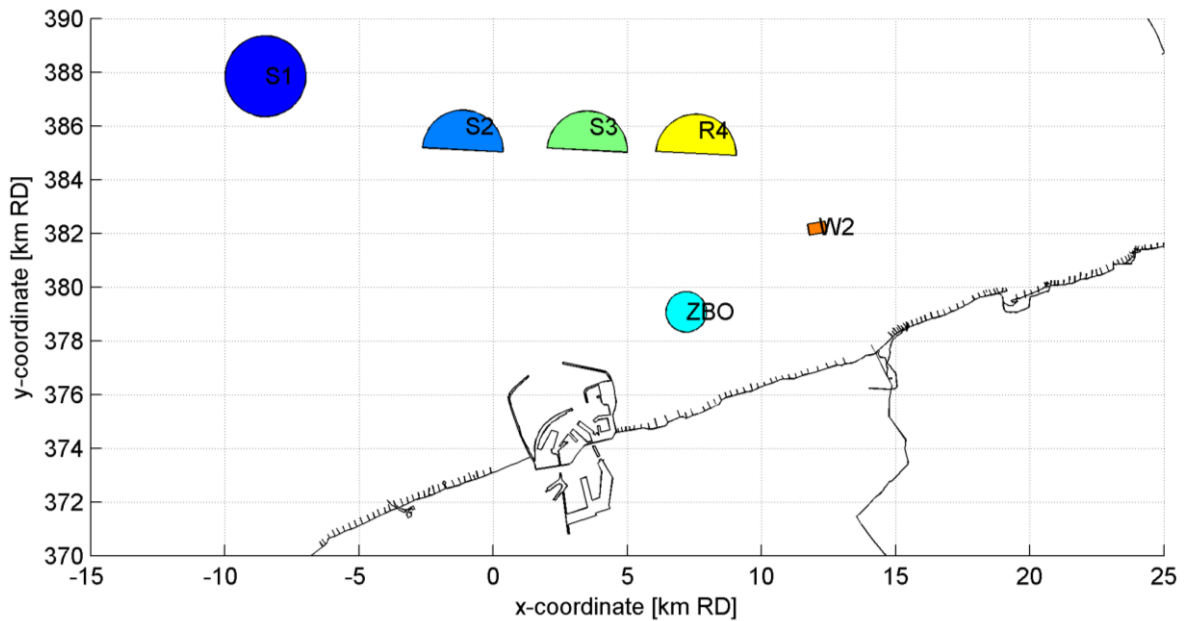


Figure 3.3 Location of dumping areas in the shelf area (of which dumping area Zeebrugge West (ZB W) is not known and missing). Figure from Vroom 2015. The current model applies a slightly different (larger) dumping area at ZBO to induce a larger dispersion of deposited material (see also Figure 4.7).

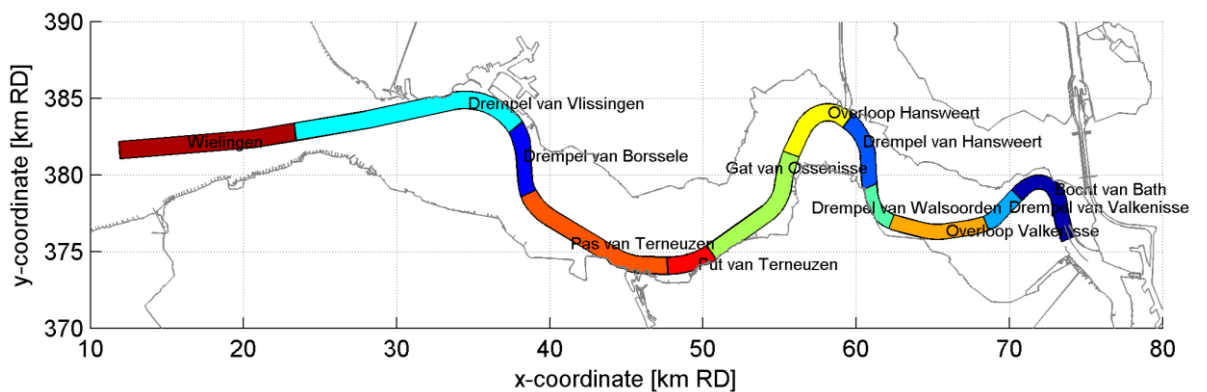


Figure 3.4 Dredging zones in the Westerschelde estuary

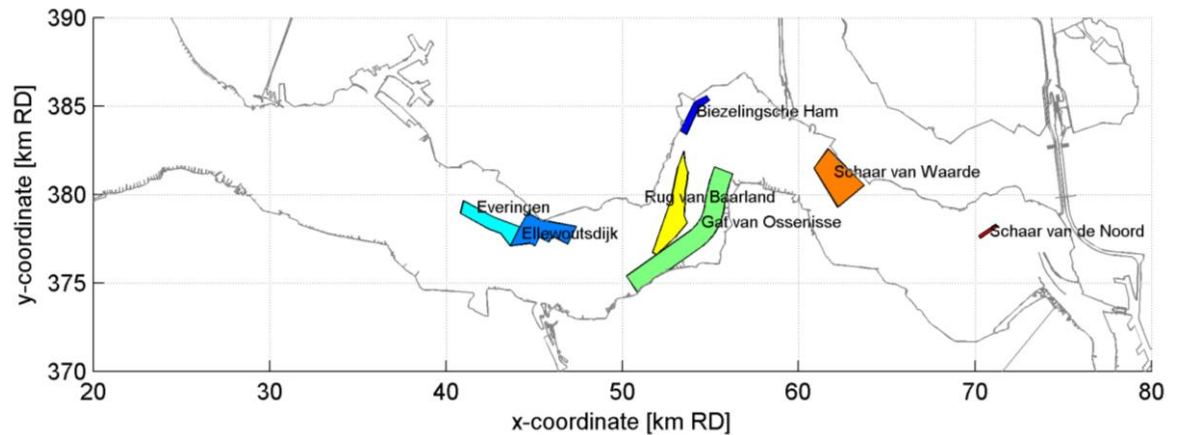


Figure 3.5 Dumping zones in the Westerschelde estuary

3.3.4 Other model settings and scenario overview

Each run consisted of two parts, from 1963 to (and including) 1984 and from 1984 to 2011. This was done to include the construction of new breakwaters at the Port of Zeebrugge, which were finished in 1984. The first part of the run included thin dams with the old breakwaters and the second run (starting from the bed and sediment availability of the first part) included the new breakwaters.

Limited sensitivity analysis on timestep, morphological factor and lateral bed slope factor (α_{bn}) lead to the parameter settings defined in Table 3.1. Sensitivity analysis on wave conditions showed much better performance for four wave conditions compared to 1 and 2 wave conditions. Applying 6 wave conditions led to too large computational effort. We carried out 4 runs to systematically investigate the importance of dredging and dumping activities, wave action, 3D effects and multiple, i.e. 2, sand fractions. The latter two parameters were included in a single run for reasons of time saving.

Following Van der Wegen et al. (2011), we derived the initial distribution of sediments by running the model for a month without bed level changes, but allowing for bed composition change so that finer material was washed out from channels and shoals were covered with finer sediment fractions.

Table 3.1 Most relevant Delft3D parameter settings

Parameter	Value
Dimensions	2D
Timestep	15 s
Hydraulic forcing	Nested from ZUNO model All astronomic constituents
Wave forcing	Mormerge 4 wave conditions (see Appendix and Van Rooijen (2015))
Wave communication interval	1 hour
Sediment transport formulation	Van Rijn (Delft3D default)
Sand diameter	120 μm
Lateral bed slope factor (α_{bn})	100
Erosion of adjacent dry cells	on
Dredging activities	Time dependent following Vroom et al. (2015a). For locations see Figure 3.2, 3.3., 3.4 and 3.5. The dumping area directly east of Zeebrugge was enlarged compared to previous studies to prevent too strictly allocated deposition.
Non-erodible layers	Based on Grasmeijer et al. (2013)
Roughness	Manning, landward stepwise varying from 0.024 at sea to 0.029 $\text{s/m}^{1/3}$ near Antwerp, based on 2006 data calibration by Grasmeijer et al. (2013)
Timestep	15 sec
Hydraulic runtime	73 days
Morphological factor	104
Morphological runtime	21 years (1963–1984)

Table 3.2 Scenario overview

	Wave conditions	Dredging and dumping included	Number of dimensions	Number of sediment fractions	Run duration for 1963-2011 period	
					Wall clock (hrs)	CPU (hrs)
Run 1	4	Yes	2D	1 (120 μm)	300	750
Run 2	0	Yes	2D	1 (120 μm)	184	650
Run 3	4	No	2D	1 (120 μm)	323	1100
Run 4	4	Yes	3D	2 (200, 400 μm)	1800	2760

4 Results

4.1 Hydrodynamic validation

The model underestimates the M_2 tidal amplitude in the entire basin varying from about 10 cm, 7%, at Westkapelle to about 30 cm, 15% near Antwerp (Figure 4.5). The probable reason is that we applied Manning roughness values resulting from a calibration effort on 2006 data and bathymetry (Grasmeijer et al., 2003). Starting from 1963, these roughness values lead to a bathymetry that is probably too shallow resulting in higher tidal wave dissipation rates. The increasing trend of the tidal amplitude at Antwerp measured between 1989 and 2012 is captured by the model. Figure 4.6 shows that the M_2 phase differences along the Westerschelde are similar to observed phase differences

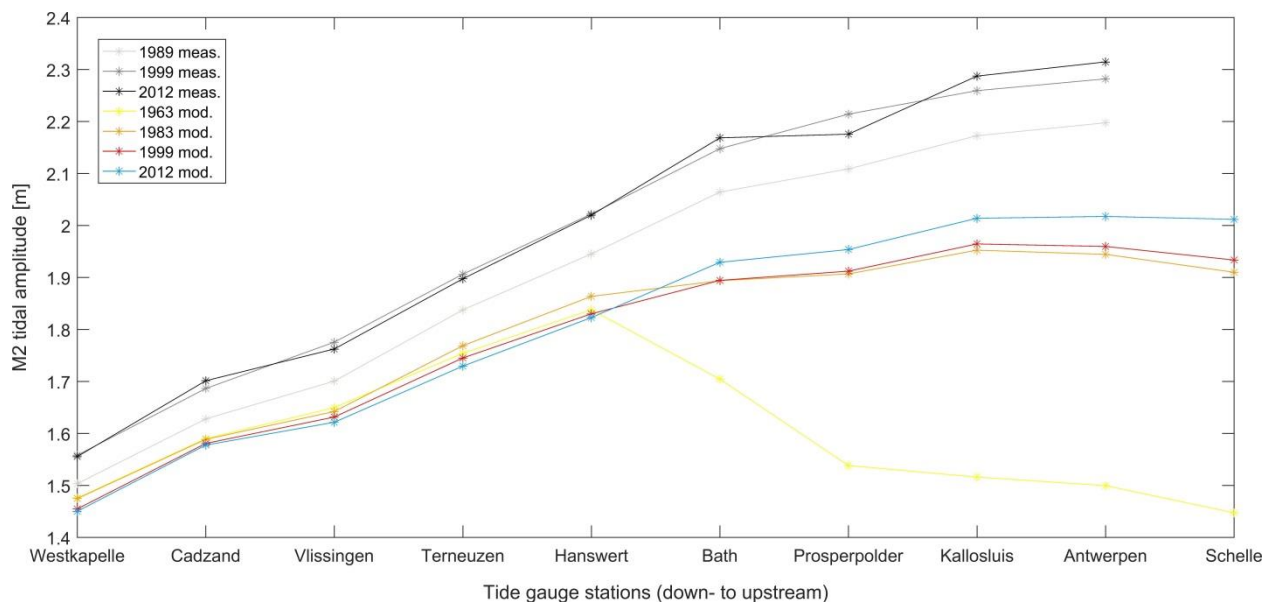


Figure 4.1 Tidal amplitudes at different stations from Westkapelle upstream to Schelle in the period 1963–2012.

Graphs in grey to black show the amplitudes based on measured tide gauge data, whereas the coloured graphs indicate the amplitudes derived from model data. As there was no consistent measured data available for 1963, tidal amplitudes were plotted for the year 1989 instead.

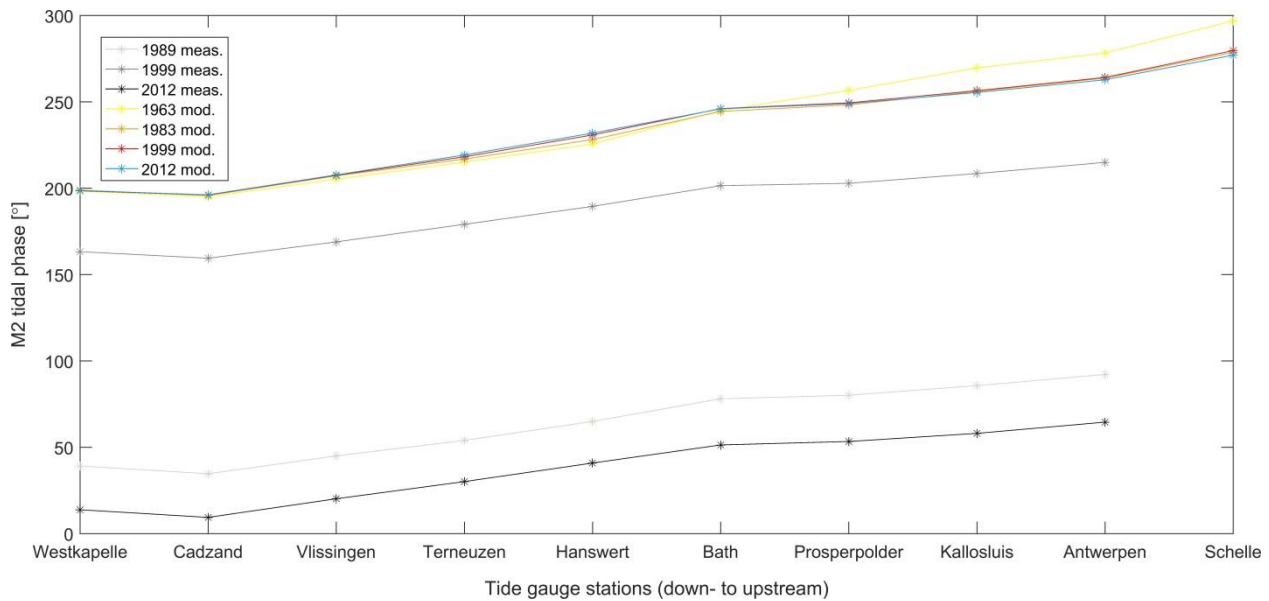


Figure 4.2 Tidal phases at different stations from Westkapelle upstream to Schelle in the period 1963–2012. Graphs in grey to black show the phases based on measured tide gauge data, whereas the coloured graphs indicate the phases derived from model data. As there was no consistent measured data available for 1963, tidal phases were plotted for the year 1989 instead.

4.2 Trends in bathymetric development

Figure 4.3 shows observed and measured bathymetries over the 1963-2011 period, while a complete sequence of this period can be found in Appendix B. The 3D model leads to best results. Observations (Figure 4.4) show that the Rassen shoal moves landward (black arrow) squeezing the Geul van de Rassen. At the same time the connecting channel between Deurloo West and Geul van de Rassen becomes shallower connecting the Rassen with the Elleboog (black dotted line). The model also shows the landward moving Rassen (black line) even to the extent that the Rassen merges with the Elleboog (black dotted line). Measured developments show clearly that Deurloo West and Geul van de Walvisstaart develop (red arrows) towards each other. Deurloo West disappears in the 2D model while it maintains position in the 3D model together with the Geul van de Walvisstaart. The shallow ridge developing North of the Wielingen (red dotted line) is apparent in the model results while the 3D model reproduces dynamics at the connection between Wielingen and Geul van de Walvisstaart better than the 2D model (red circle).

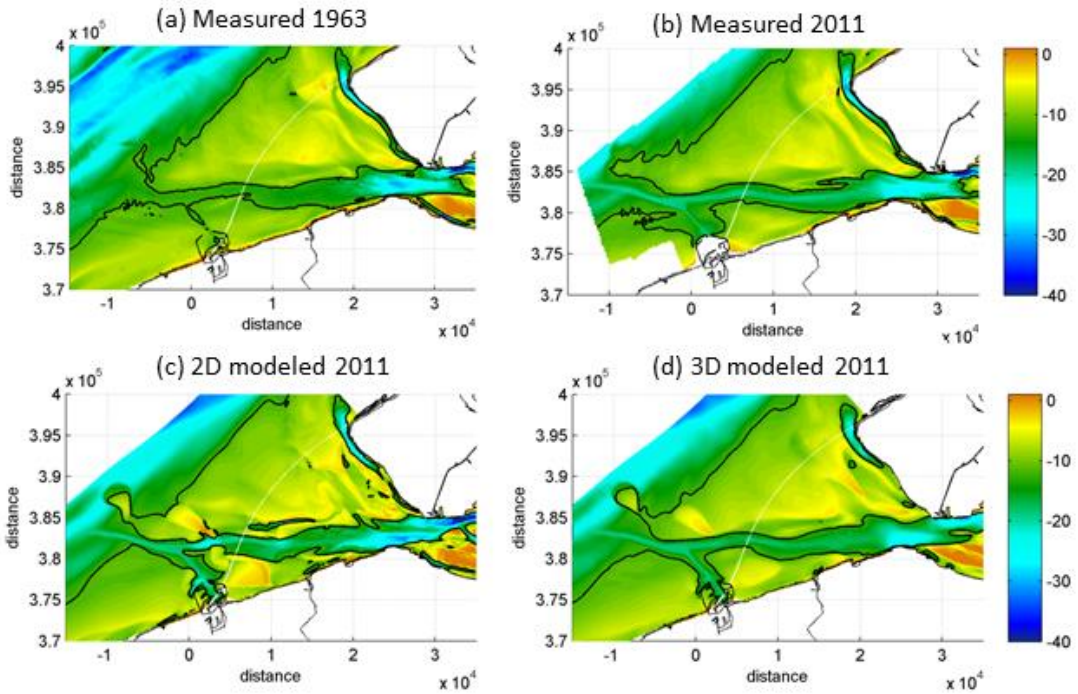


Figure 4.3 Measured (a,b) and modelled (c,d) mouth bathymetries

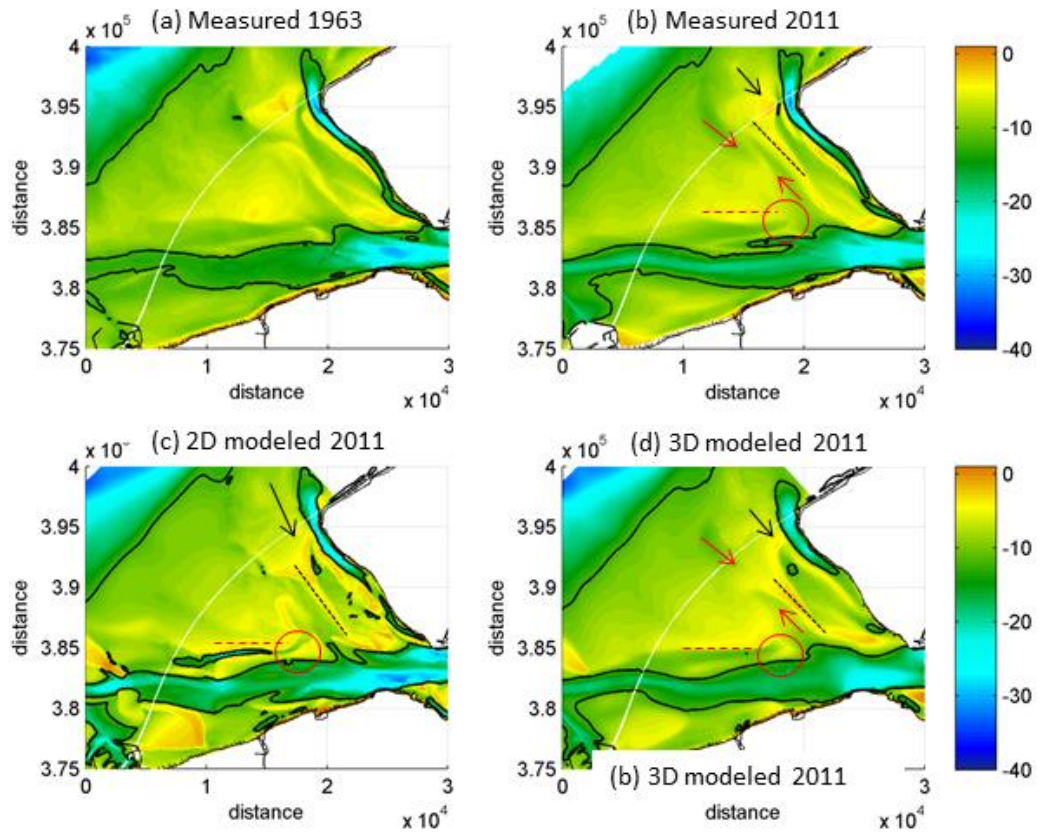


Figure 4.4 Measured (a,b) and modelled (c,d) mouth bathymetries (detailed).

4.3 Erosion and sedimentation patterns

We use the 2D model results as starting point for the sensitivity analysis. The cumulative erosion and sedimentation patterns (Figure 4.5 with details in Figure 4.6) show resemblances and differences with observations. Generally, largest developments take place in the Westerschelde itself. The morphodynamic development at the mouth is less in 3D than in 2D. The patterns in the landward portion (between x-coordinates 50 and 70 km) are quite well represented. The erosion patterns in the middle part (between x-coordinates 25 and 50 km) resemble quite well but deposition is overestimated largely in areas where dumping is defined (areas SN11, SN31, HP1 and HP3), see also Figure 4.7. The patterns at the mouth (between x-coordinates -10 and 25 km) show that the access channels can be well recognized. The pronounced deposition between km -10 and -15, North of the Port of Zeebrugge and at the eastern side of the Zeebrugge breakwaters is the result of dumping activities. Between y-coordinates 38 and 38.5 km and x-coordinates 10 and 25 km new channels develop and pronounced erosion and deposition occurs in the Wielingen close to the shore line, which is not observed in reality. More northward, between y-coordinates 38.5 and 39.5 km, patterns are reflected quite nicely, albeit that there is also a strange local convergence of deposition directly northwest of the Geul van de Rassen. The Oostgat and the Geul van de Walvisstaart both erode while measured deposition at the Elleboog and Het Bankje van Zoutelande is reflected by the model.

In general, modeled deposition volumes by dredging activities cause quite distinct deposition patterns (e.g. east of Zeebrugge breakwaters and south of Vlissingen) which in reality are much more dispersed due to the more gradual (in time) and diverged (in space) dumping activities. The 3D model leads to more diffuse patterns and performs better.

Figure 4.8 clearly demonstrates the impact of waves and dredging activities on the mouth morphodynamics. Without waves the developments around the Oostgat and Geul van de Rassen are not well represented and dumped material remains at its dumping location in shallower parts. Excluding dredging activities (but including waves) seems to have a higher impact on the morphodynamics than excluding waves. It leads to the development of considerable deposition in the "Scheur" in front of Zeebrugge Port and a smaller spit-like bar in the Wielingen, more eastward.

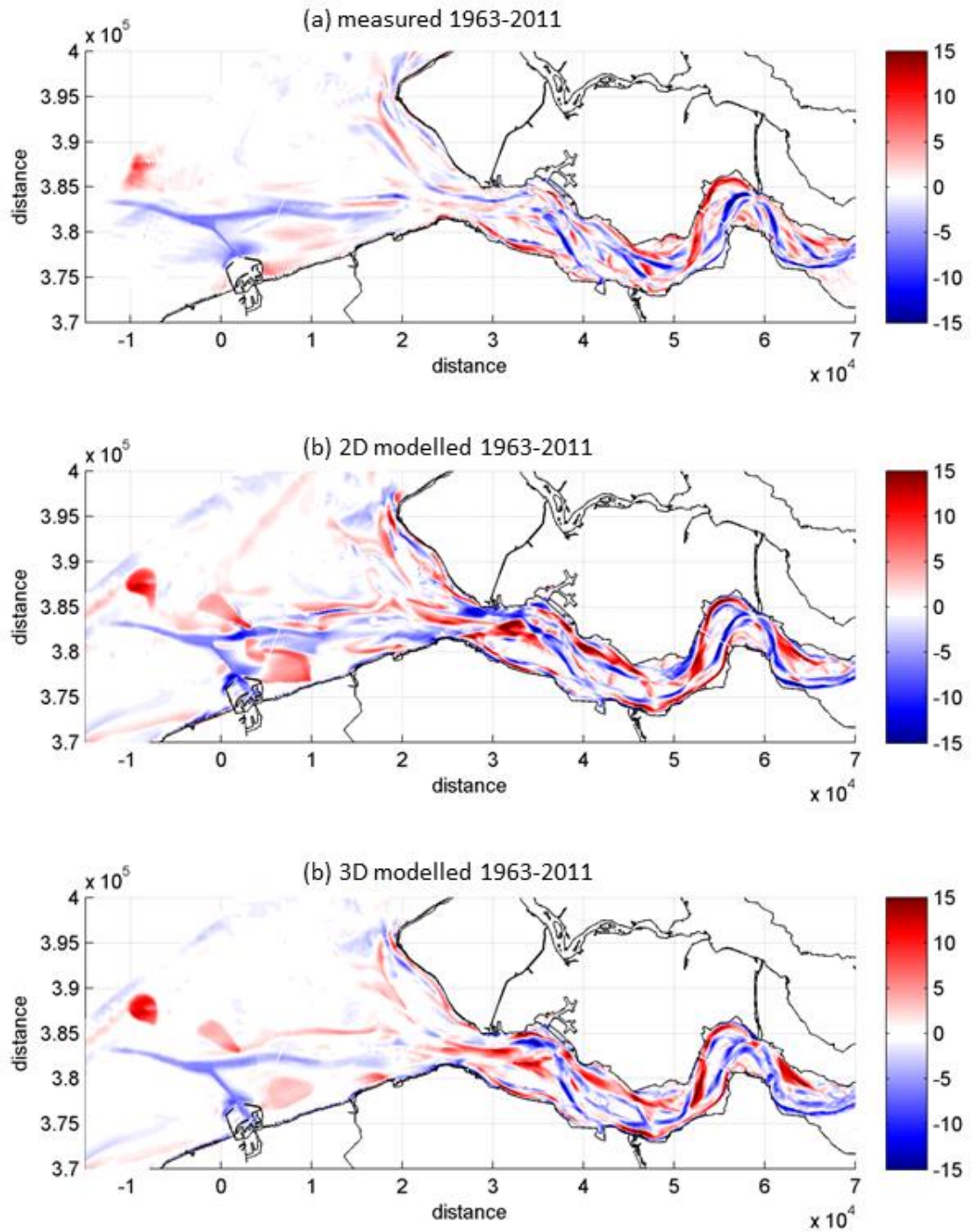


Figure 4.5 Cumulative erosion and sedimentation patterns (in m) between 1963 and 2011 of (a) measurements and (b) 2D model results and (c) 3D model results.

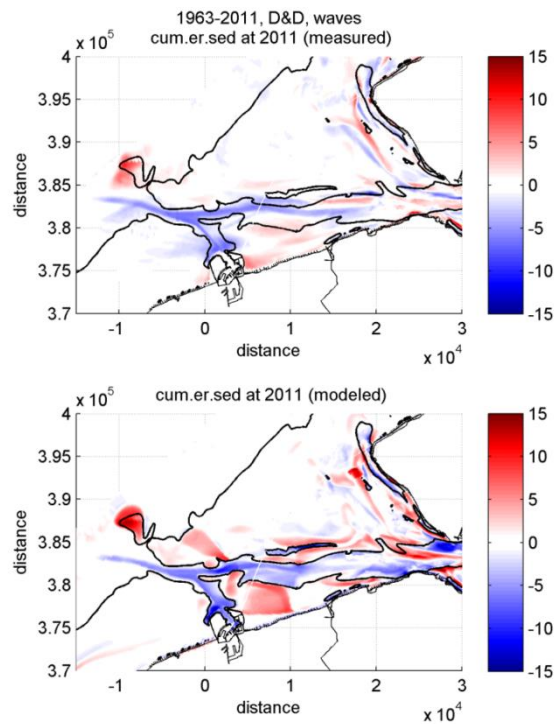


Figure 4.6 Detail of Figure 4.5 Cumulative erosion and sedimentation patterns (in m) between 1963 and 2011 of measurements (upper panel) and model results (lower panel). Contour lines show the 2011 modelled bathymetry at 12m-MSL.

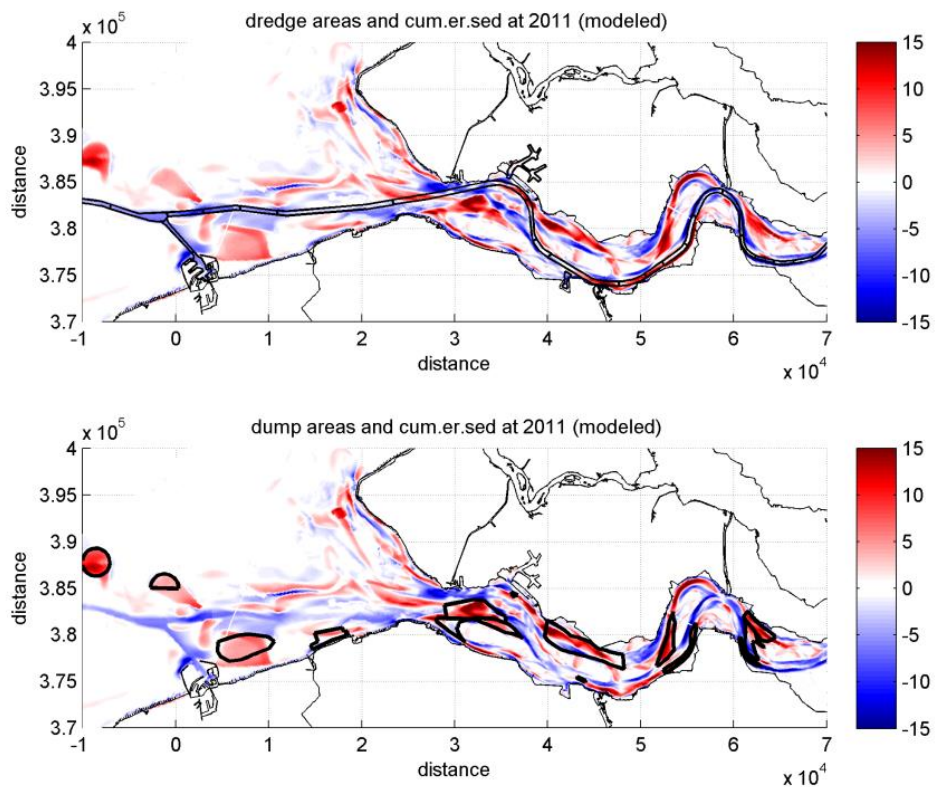


Figure 4.7 Modeled cumulative erosion and sedimentation patterns (in m) between 1963 and 2011 including dredge areas (upper panel) and dump areas (lower panel). The dumping area directly east of Zeebrugge was enlarged compared to previous studies to prevent too strictly allocated deposition.

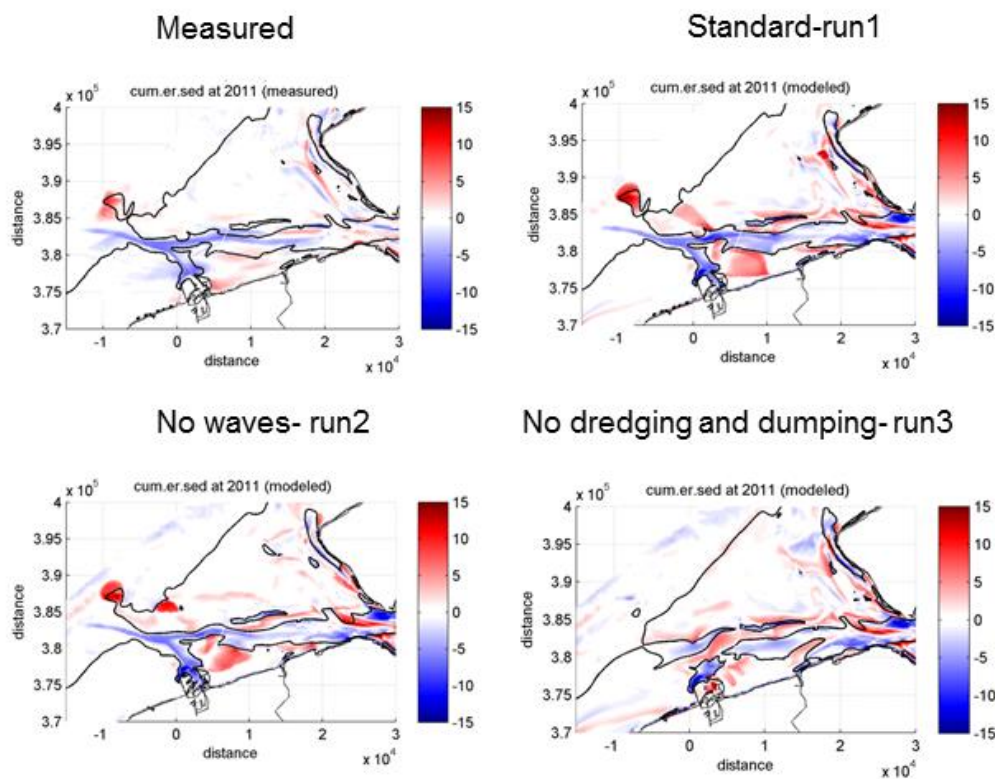


Figure 4.8 Measured (upper left) and modelled (other panels) cumulative erosion and sedimentation patterns (in m) between 1963 and 2011 including waves and dredging and dumping (upper right panel), excluding waves (lower left) and excluding dredging and dumping (lower right). Contour lines show the 2011 modelled bathymetry at 12m-MSL.

4.4 Skill scores

The skill scores are low and mostly negative (Figure 4.9) but generally show an increasing trend, even leading to positive scores in 2011. The landward area performs best, followed by the mouth area. BSS increases slightly if we compensate for bathymetric measurement errors of 0.5m following Van Rijn (2003), see also Appendix B (see Figure 4.9b) or do not consider bed level changes of less than 0.5m in calculating the BSS (Figure 4.9c). After 1984 the BSS seems more constant, which maybe related to the impact of dredging activities (see also Section 4.6).

We expect the skill scores to be low because morphodynamic models typically need a morphological spin up of decades (Dam et al. 2013 and Figure 1.4). The impact of dredging from 1984 onwards has a positive effect on the skill scores (sudden increase of blue lines in 1984 in Figure 4.9) suggesting that dredging impact is large compared to autonomous development. Model results also confirm that the part constrained in width (landward part) performs better than the wider mouth, although the middle part performs worse than the mouth part. Runs without waves perform slightly worse (although the mouth area performs initially better!), while excluding dredging activities leads to worse BSS. Tidal movement and dredging activities play a larger role in the mouth morphodynamics than wave action. 3D runs show the best, almost continuously positive trend (Figure 4.10).

We investigated more closely whether BSS was location dependend (some locations performing better than others) or depth dependend (some depth classes performing better than other depth classes), see Figure 4.11 and Figure 4.12.

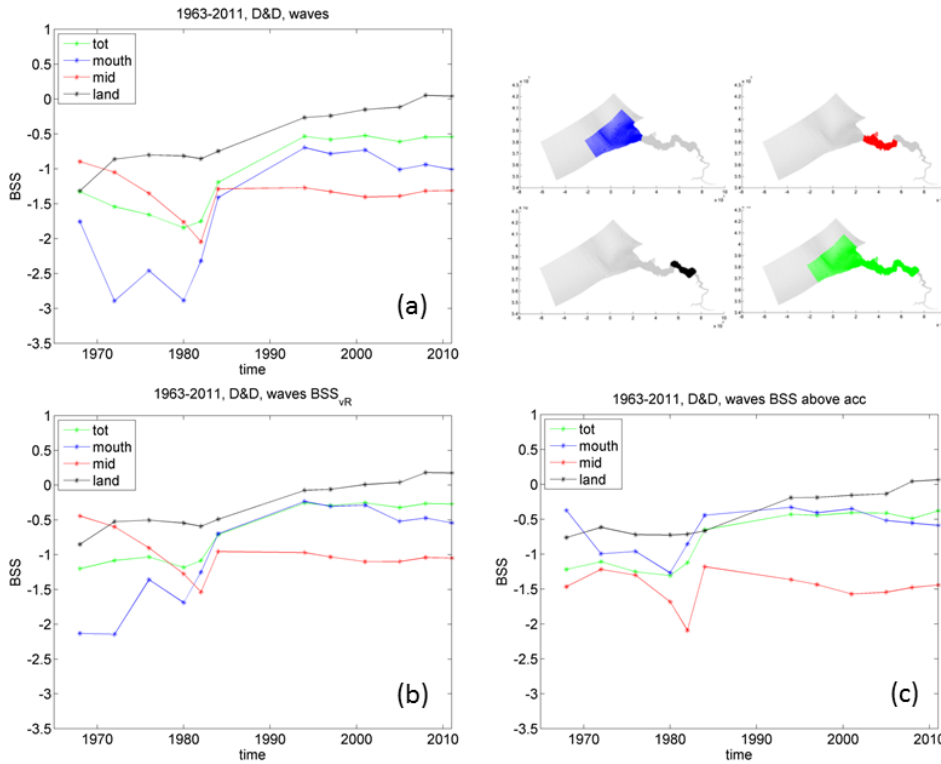


Figure 4.9 Run 1 (a) Brier Skill Scores; (b) BSS corrected for measurement accuracy of 0.5m; (c) BSS not including bed level changes of less than 0.5m.

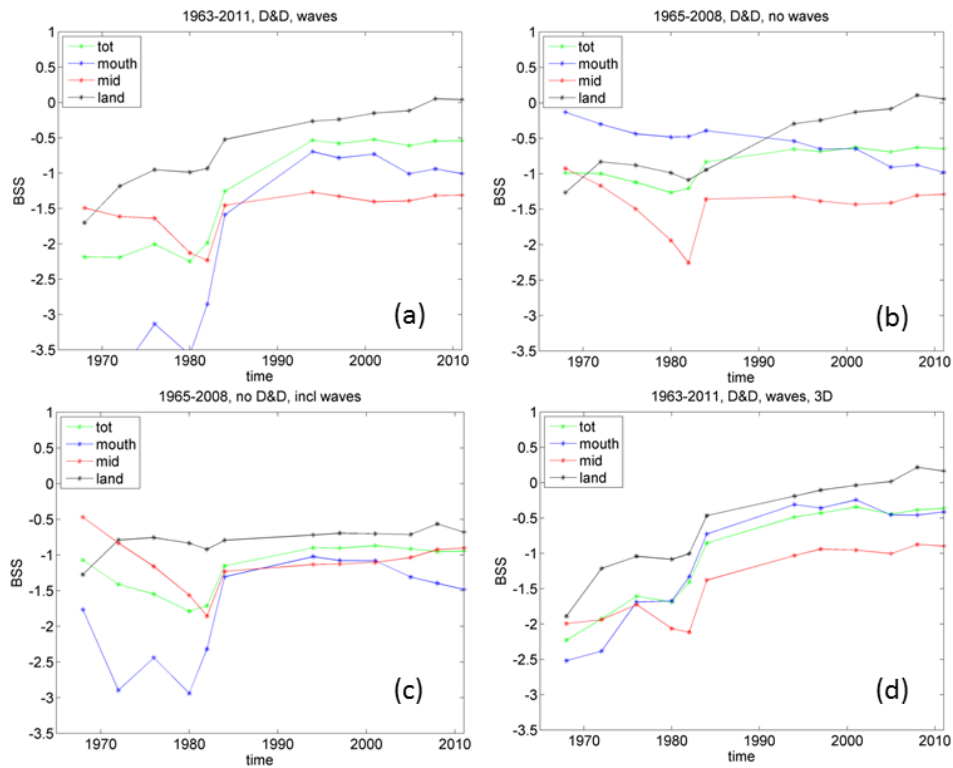


Figure 4.10 (a) Brier Skill Scores, Run 1; (b) BSS without waves, Run 2; (c) BSS not including dredging activities, Run 3; (d) BSS 3D with waves and dredging activities, Run 4.

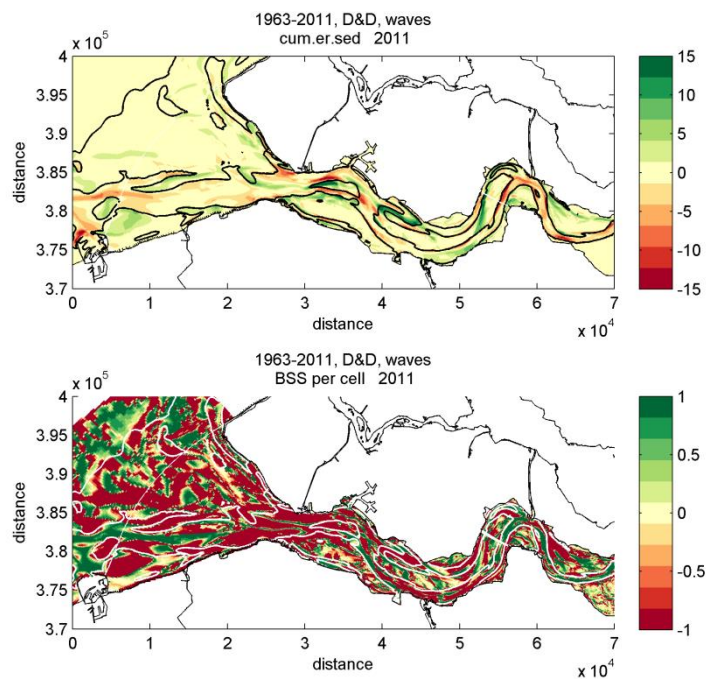


Figure 4.11 (a) Erosion and sedimentation patterns over the 1963-2011 period, Run 1; (b) BSS in 2011 per gridcell.

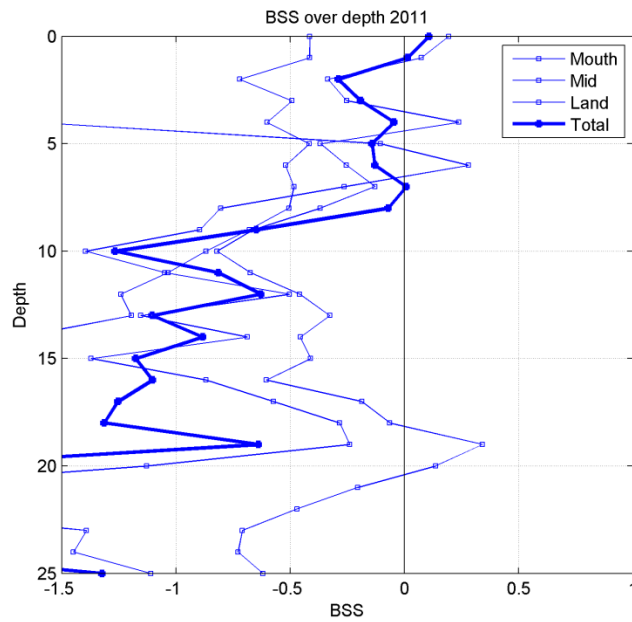


Figure 4.12 BSS per depth (1 m bins) for different domains over the 1963-2011 period, Run 1.

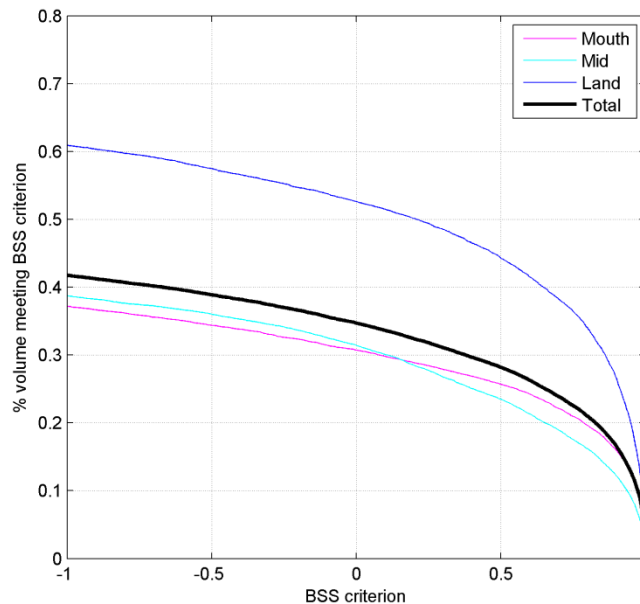


Figure 4.13 % of erosion and sedimentation volume meeting BSS criterion.

The BSS showed a rather scattered result over the domain and over the depth classes with no significant trends over time, implying that the BSS did not depend on location or depth class. Remarkably, the BSS for some locations and depth classes was very good (between 0.5 and 1), which was obviously compensated with worse BSS in calculating the overall (depth and domain integrated) BSS (e.g. Figure 4.9). Figure 4.13 shows the total erosion and sedimentation volume meeting a specific criterion. For example, about 45% of the modeled erosion and sedimentation volume in the land domain meets the criterion of $BSS \geq 0.5$. The

figure confirms the outperforming land domain and corresponds to values and trends found by Van der Wegen and Jaffe (2013) for the decadal morphological hindcast of an inland tidal embayment in San Francisco Estuary.

4.5 Sediment availability

The sediment thickness for the Westerschelde mouth in Figure 2.2 was derived from low resolution coring and the fact that major shallow parts just have not been incised by channels historically. Figure 4.14 shows the sediment availability sometimes reducing to none in large parts of the mouth. However, Van der Spek (personal communication) suggests that large parts of the Westerschelde mouth should be sandy. We started runs that included a larger sediment availability of 50 m in the mouth, but these became unstable around 1990. Comparison of results until 1990 showed only minor differences between standard Run 1, indicating that sediment availability has a minor effect.

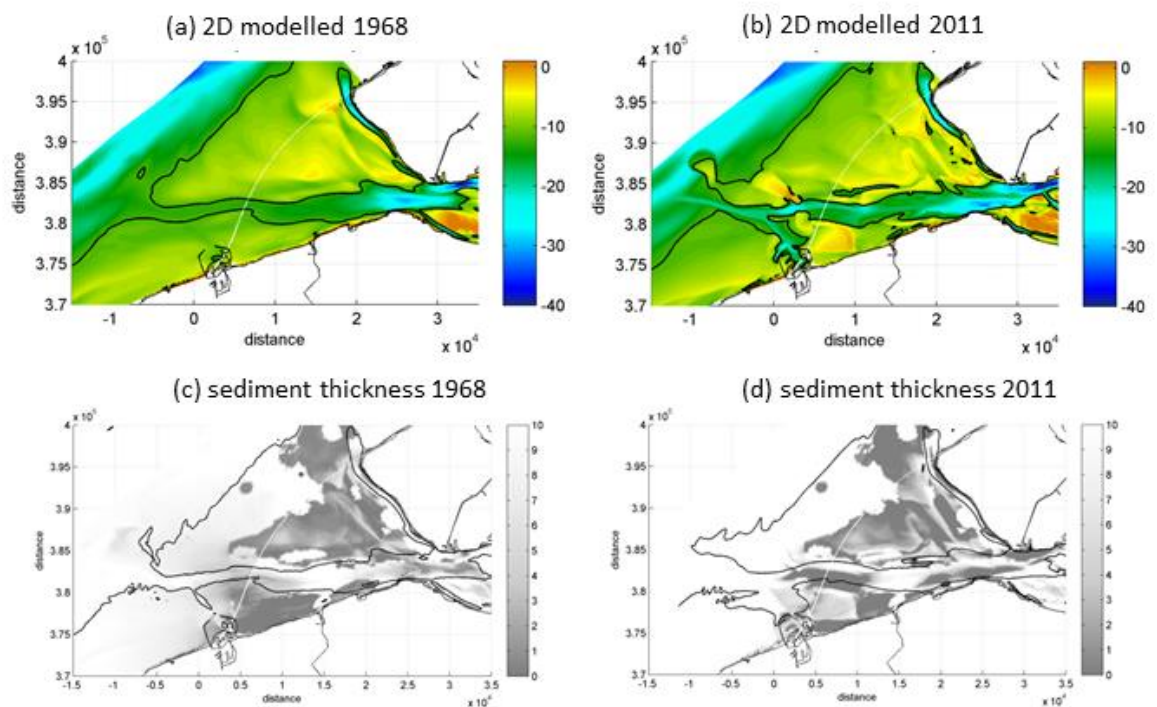


Figure 4.14 Standard run 1 (a,b) modelled bathymetries in 1968 and 2011 and (c,d) modelled sediment thickness in 1968 and 2011

4.6 Dredging and dumping volumes

Figure 4.15 compares the modeled and measured (Vroom et al., 2015a) dredging volumes. Volumes in the Scheur correspond quite nicely (a volume difference of about 10%). The volumes in the Wielingen and the Geul are comparatively small, but are overestimated by the model almost by a factor 2. The largest difference occurs at the Pas van Zand where the model highly underestimates the dredged volume. This is attributed to the sediment characteristics being muddier in the Pas van Zand than at other locations. A model that includes mud dynamics would probably perform better. Dredging volumes from 3D runs and 2D runs without waves are comparable, although the 3D model highly overestimates dredged volumes in the mid region (more specifically in the Gat van Ossenissee). Appendix D provides more detailed dredging activity model results in the Westerschelde itself.

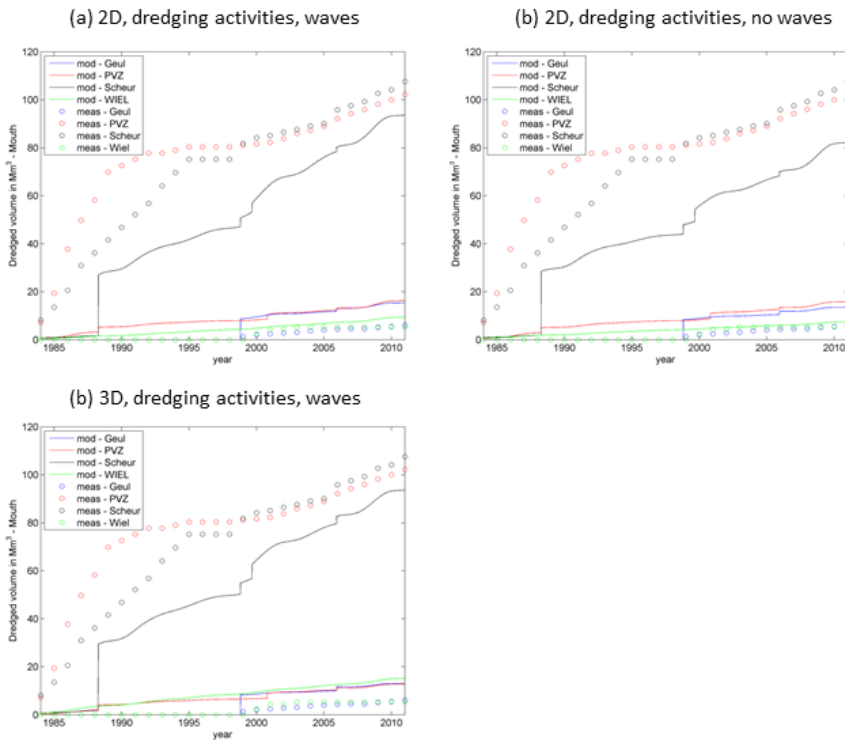


Figure 4.15 Dredged volumes from the mouth (see Figure 3.2 for locations)

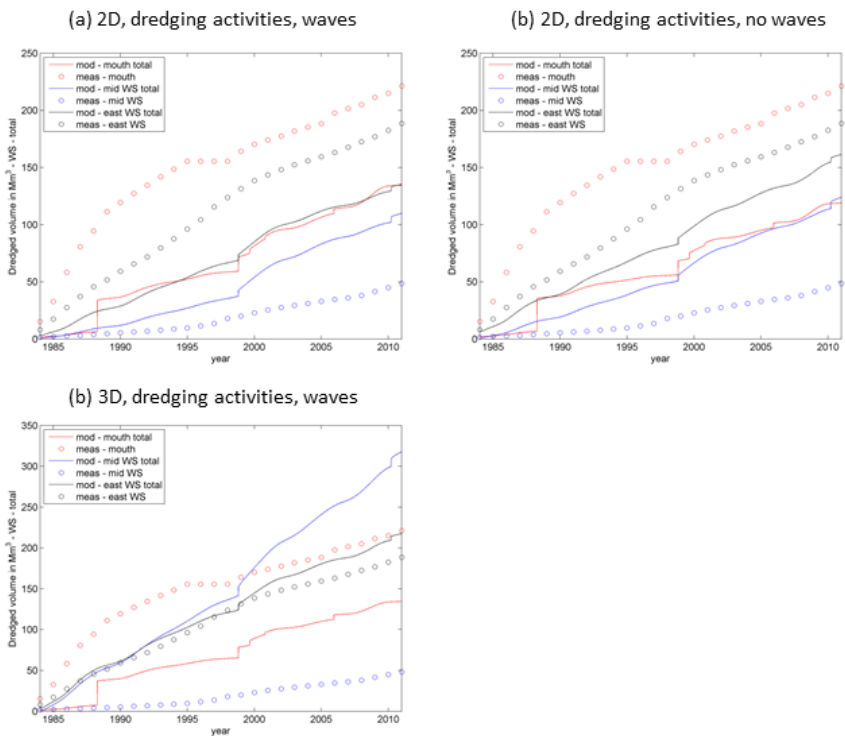


Figure 4.16 Dredged volumes from the entire Westerschelde (see Figure 4.9 for locations)

5 Discussion and conclusions

This work gives an indication of what can be accomplished with Delft3D type of modeling work for decadal time scale morphodynamic predictions in the Westerschelde mouth.

Generally, the 3D, 2 sand fractions model produces more diffuse results that compare better with observations than the 2D model. An example is the shoal developing eastward of the Port of Zeebrugge as the result of dumping activities, which is quite pronounced with sharp bed level gradients in case of 2D and more diffuse in case of the 3D run. The reason why the dumped volumes east of Zeebrugge Port do not disperse well (in both 2D and 3D runs), is that finer material (the deposited material is supposedly mud) is not considered in this model. Similarly, Pas van Zand dredging volumes are not well captured since our model excludes mud.

Overall, modelled erosion and sedimentation patterns reflect main developments in the mouth over the 1963-2011 period. Model performance is better in 3D with two sand fractions compared to 2D with a single sand fraction, in the (more confined) Westerschelde itself and on longer time scales. Sensitivity runs excluding waves or dredging activities lead to less performance and indicate where waves or dredging activities have a large impact. In general, dredging activities have a larger impact than wave action. Still, the major forcing steering morphodynamic development of the Westerschelde mouth is the tidal movement itself.

Dam et al. (2016) reached positive skill scores for the inner part of the Westerschelde after 30 years. Our model reaches positive skill scores after 50 years and only in the inner parts. A possible reason is that the mouth morphodynamics is governed by more complex processes (e.g. wave action and sediment composition) that requires more subtle process schematization. A possible reason for the weaker score in the inner parts of the Westerschelde is that Finel, due to its numerical scheme, is more diffuse than Delft3D. This diffusivity may work as a compensation for processes not accounted for such as bed slope effects or multiple sediment fractions (in case of the Finel modeling study by Dam et al. (2016) or effects related to the forcing schematisation (wave conditions, extreme events). Increasing the diffusion coefficient in Delft 3D in long term runs could thus increase model skill.

Closer analysis suggests that sediment composition plays an important role. For example, Figure 5.1(b) shows that suspended sediment transports in 2D are twice as high as the sum of the two suspended sediment fractions in 3D at Bol Knokke at the edge of the Wielingen and the Vlakte van de Raan. This can be explained by the fact that the sand fractions (200 and 400 μm) in the 3D run are larger than in the 2D run. Similarly, the bed load in 2D is about 2.5 times smaller than the combined bed load of the two fractions in 3D. The bed slope factor is an important parameter influencing morphodynamics with a larger factor leading to more diffusive results. Since the bed slope factor only affects the bed load magnitude and direction its effect is larger in the 3D runs.

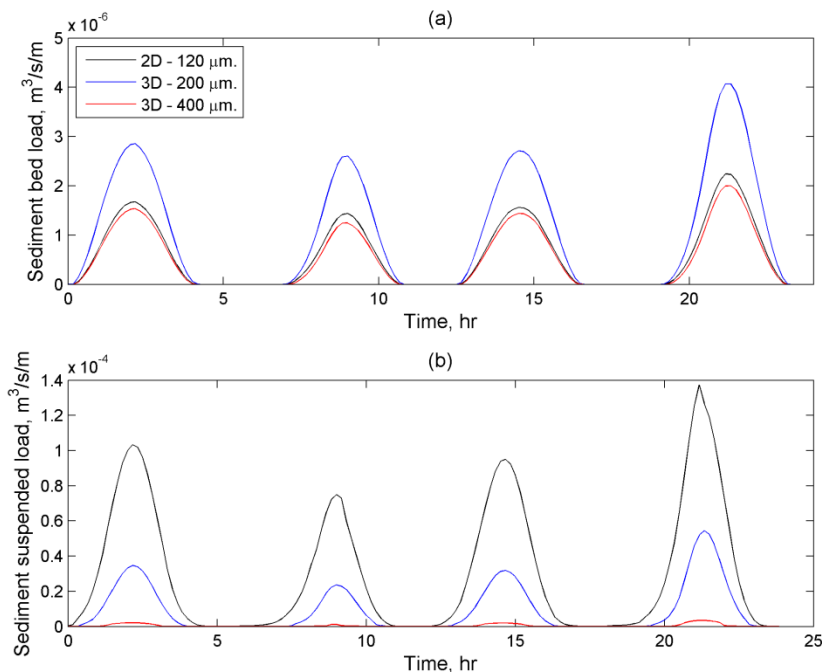


Figure 5.1 Sediment bed load (a) and sediment suspended load (b) at Bol Knokke (North of Knokke at northern Wielingen channel side at 8.5 m waterdepth) for 2D ($D=120\ \mu\text{m}$) and 3D ($D=200$ and $400\ \mu\text{m}$) runs.

The computational time is long (~ 10 days), which limits more sensitivity analysis and further optimisation of model results. Adding more dynamics and complexity (3D, multiple sediment fractions, e.g. mud) significantly increases computational time (about 70 days for 3D with two sediment fractions).

This study provides an overview of how process-based modeling efforts can contribute to predict decadal time scale morphodynamic developments in the Westerschelde mouth. The hindcasted morphodynamic developments are less and require more subtle process descriptions than the tide dominated and confined inner parts of the Westerschelde. Model results indicate the relative importance of wave action, dredging activities, sediment fractions, dimensionality (i.e. 2D vs 3D) and tidal action. Although model results differ from observations, model skill becomes better over time and do not lead to seemingly unrealistic or unstable developments.

Model runs could be extended beyond 2011 giving more trustworthy results than starting from a 2011 bathymetry. These predictions can be carried out including interventions such as the dredging of the Geul van de Walvisstaart into an access channel. A process-based modelling effort assessing the impact of such an intervention would be more convincing when the intervention measures are large compared to the autonomous development of the system. Starting from a hindcasted bathymetry or starting from a measured bathymetry would in such as case be of limited importance.

6 Future work

A more extensive sensitivity analysis should be carried out to optimise model performance. Important variables are bed slope factor, including multiple fractions of both sand and mud, more complex wave schematisations. Van der Spek (personal communication) suggests that large parts of the Westerschelde mouth should be sandy. Runs that include a larger sediment availability became unstable after 1990. Although these runs did not show a major difference, it would be worthwhile finishing the runs with smaller time steps to come to firmer conclusions.

Further sensitivity analysis would be justified given the sensitivity of the model results to sediment fractions and (expected) the bed slope factor. A coarser model would benefit more straightforward sensitivity analysis at the cost of spatial resolution. However, the optimised model settings can be used in a next step to feed limited additional runs with the high resolution NeVla model. E.g. inclusion of mud seems to be essential to capture dredging volumes at the mouth, but maybe also within the Westerschelde. We need to get a better grip on how mud performs on long-term morphodynamic predictions, e.g. in terms of spin-up, sediment characteristics and supply. Schematized modelling with coarser models would provide a good strategy to explore mud morphodynamics before applying this in large NeVla type of models.

The 3D run with 2 sediment fractions leads to best results. We think that this is partly due to the 3D spiral flow effects, but the inclusion of two sediment fractions may also have a governing role. The impact of including multiple sediment fractions ideally should be assessed in separate runs.

7 References

- Cleveringa, J., (2006). Morphodynamische ontwikkeling Voordelta. Rapport Alkyon A1698.
- Cleveringa, J., (2008). Morphodynamics of the Delta coast (south-west Netherlands). Quantitative analysis and phenomenology of the morphological evolution 1964-2004. Rapport Alkyon A1881.
- Cleveringa (2013). Grootschalige sedimentbalans van de Westerschelde. Project LTV Veiligheid en Toegankelijkheid; LTV V&T-RAPPORT K-17. Rapport 076945827:0.4 – Definitief, Arcadis.
- Dam, G., et al. (2013), Actualisatie van het FINEL2d model van de Westerschelde ten behoeve van Lange Termijn Visie Scheldeestuarium, Veiligheid en Toegankelijkheid, A26; 1630/U11274/GD/G.
- Dam, G., M van der Wegen, RJ Labeur, D Roelvink (2016), Modeling centuries of estuarine morphodynamics in the Westerschelde estuary, *Geophysical Research Letters* 43 (8), 3839-3847
- Damen, J. (2014). Coastward erosion of tidal channel Oostgat. Afstudeerverslag, Universiteit Twente.
- Dissanayake, D.M.P.K., Roelvink, J.A., Van der Wegen, M., 2009b. Modelled channel patterns in a schematized tidal inlet. *Coastal Engineering* 56, 1069–1083.
- Elias and Van der Spek (2015), Grootschalige morfologische veranderingen in de Voordelta
- Erkens, G. (2003). Analyse Multibeam data Oostgat. (102 p.). Den Haag: Rijksinstituut voor Kust en Zee.
- Fettweis, M., and Van Den Eynde, D., (2003). The mud deposits and the high turbidity in the Belgian-Dutch coastal zone, southern bight of the North Sea. *Cont. Shelf Res.* 23, 669–691.
- Fettweis, M., Nechad, B., and Van den Eynde, D., (2007). An estimate of the suspended particulate matter (SPM) transport in the southern North Sea using SeaWiFS images, in situ measurements and numerical model results. *Cont. Shelf Res.* 27, 1568–1583.
- Fettweis, M., Francken, F., Van den Eynde, D., Verwaest, T., Janssens, J., and Van Lancker, V., (2010). Storm influence on SPM concentrations in a coastal turbidity maximum area with high anthropogenic impact (southern North Sea). *Cont. Shelf Res.* 30, 1417–1427.
- Grasmeijer et al. (2013), Actualisatierapport Delft3D Schelde-estuarium ten behoeve van Lange Termijn Visie Scheldeestuarium, Veiligheid en Toegankelijkheid, A27; I/RA/11387/12.103/GVH
- Lauwaert, B., Bekaert, K., De Brauer, D., Fettweiss, M., Hillewaert, H., Hoffman, S., Hostens, K., Mergaert, K., Moolaert, I., Parmentier, K., and Verstraeten, J., (2006). Syntheserapport over de effecten op het mariene milieu van baggerspeciestorringen (vergunningperiode 2004-'06).
- Murphy, A.H., and E.S. Epstein (1989), Skill scores and correlation coefficients in model 890 verification, *Monthly Weather Review*, 117, 572–581.
- Sutherland, J., A.H. Peet, and R.L. Soulsby (2004), Evaluating the performance of morphological models, *Coastal Engineering*, doi:10.1016/j.coastaleng.2004.07.015
- Sha, L.P., 1989. Variation in ebb-delta morphologies along the West and East Frisian Islands, The Netherlands and Germany. *Marine Geology* 89, 11–28.
- Steijn, R., and Van der Spek, A., (2005). Mogelijkheden voor geulwandversterking of verlegging Oostgat/Sardijneul, Verslag van bureaustudie. Rapport A1431. Alkyon, Nederland.
- Tonnon, P.K., and van der Werf, J., (2014). Geulopdringing Zuidwest Walcheren, Deltares report 1208921-000-ZKS-0005.

- Van der Slikke, M.J. (1997). Grootchalige zandbalans van de Westerscheldemonding (1969-1993), een inventarisatie van dieptegegevens (1800-1996). Rapport R97-18, IMAU, Utrecht.
- Van der Wegen, M., and B. E. Jaffe. "Towards a probabilistic assessment of process-based, morphodynamic models." *Coastal Engineering* 75 (2013): 52-63.
- van der Wegen, Mick, et al. "Bed composition generation for morphodynamic modeling: case study of San Pablo Bay in California, USA." *Ocean Dynamics* 61.2-3 (2011): 173-186.
- Van der Werf, J., and Brière, C., (2013). Influence morphology on tide and sand transport: Basisrapport grootchalige ontwikkeling G-4, Deltares report 1207720-000.
- Van Enckevoort, I., (1996). Morfologisch onderzoek Westerscheldemonding; deel 2 Morfologische ontwikkeling van de Westerschelde monding sinds 1800, Universiteit Utrecht IMAU rapport R 96-21.
- Van Kessel, T., Vanlede, J., and de Kok, J., (2011). Development of a mud transport model for the Scheldt estuary. *Cont. Shelf Res.* 31, S165–S181.
- Van Oyen, T.; Van der Vegt, M.; De Maerschalck, B.; Nnafie, A.; Verwaest, T.; Mostaert, F. (2016). Improving long-term morphological modelling tools: Subreport 1 – Literature Review: morphology of the Scheldt estuary mouth. Version 4.0.
- WL Rapporten, 14_094. Flanders Hydraulics Research, Antwerp, Belgium.
- Van Rooijen, A. (2015), Afleiding golfklimaat Westerschelde project (memo)
- Van Rijn, L.C., 1997. Sediment transport and budget of the central coastal zone of Holland. *Coastal Engineering* 32, 60 – 90
- Van Rijn, L. C., D. J. R. Walstra, B. Grasmeijer, J. Sutherland, S. Pan, and J. P. Sierra (2003), The predictability of cross-shore bed evolution of sandy beaches at the time scale of storms and seasons using process-based profile models, *Coastal Eng.*, 47, 295–327, doi:10.1016/S0378-3839(02)00120-5.
- Van Veen, J., 1936. Onderzoekingen in de hoofden, in verband met de gesteldheid der Nederlandsche kust (in Dutch), *Algemeene Landsdrukkerij's Gravenhage*, the Netherlands.
- Verwaest, T., Delgado, R., Janssens, J., & Reyns, J. (2011, May). Longshore sediment transport along the Belgian coast. In Paper abstract submitted for the Coastal Sediments conference, Miami, US (pp. 2-6).
- Vroom, J., and Schrijvershof, R., (2015a). Overzicht van menselijke ingrepen in de Westerschelde en haar mondingsgebied in de periode 1985-2014. Deltares memo 1210301-001-ZKS-0005 40.
- Vroom, J., de Vet, P.L.M., and van der Werf, J., (2015b). Validatie waterbeweging Delft3D-NeVla model Westerscheldemonding, Deltares report 1210301-001-ZKS-0001.
- Vroom, J. Van Maren, B, Van der Werf, J., Van Rooijen, A. (2016), Zand-slib modellering voor het mondingsgebied van het Schelde-estuarium

A Derivation of wind wave climate

A.1 Introduction

This memo describes the derivation of a representative wave climate that can be used for model simulations that are part of the Scheldt Mouth project of Deltares and Flanders Hydraulics. All materials can also be found in p:\1209395-schelde\golfklimaat\.

A.2 Available data

A.2.1 Overview

Wave data is collected in the area of interest by Rijkswaterstaat, and provided online via Waterbase¹ (stations throughout the Netherlands), and the Hydro Meteo Centrum Zeeland (HMCZ, only for the province of Zeeland)². For the current study most relevant wave stations are shown in Figure A.1. Based on the location just outside of the model grid Schouwenbank (SCHB) is the preferred station. This station has been operational since 1985 (HMCZ), however, only since 2006 wave directional data is available (Waterbase). In an earlier study (Van Rijn 2012), the wave heights at Schouwenbank were combined with wave directions measured at the Europlatform, which is located at deeper water, north of the model domain. However, here we assume that the wave directional data at Schouwenbank is sufficient enough (net ~ 7 years of data) to determine a representative wave climate.

Wind data is collected on a number of stations throughout the area (Figure A.1). For this study the wind data at Vlake van de Raan (VR) and Vlissingen is used.

An overview of all data available is given in Table A.1.

Table A.1 Overview of measured wave and wind characteristics in and around the area of interest.

Parameter	Location	Source	Period
Hsig, Hmax, Tsig, Tp, Tm02	Deurloo	HMCZ-website ³	2010-2014
Hsig, Hmax, Tsig, Tp, Tm02	Schouwenbank	HMCZ-website ³	1985-2014
Hsig, Hmax, Tsig, Tp, Tm02	Scheur-West	HMCZ-website ³	1985-2014
Water level	Europlatform	Live.waterbase.nl	1983-2014
Wave height Hsig	Europlatform	Live.waterbase.nl	1983-2014
Wave period Tm02	Europlatform	Live.waterbase.nl	1983-2014
Wave direction (mean)	Europlatform	Live.waterbase.nl	1989-2014
Wind_v, wind_dir	VvdR	HMCZ-website ³	1988-2014
Wind_v, wind_dir	Vlissingen	Potwind, OpenDap, KNMI ⁴	1981-2014
Wind_v, wind_dir	VvdR	Potwind, OpenDap, KNMI ⁴	1997-2014
Wind_v, wind_dir	Vlissingen	Potwind, KNMI-website ⁵	1959-2006

¹ <http://live.waterbase.nl>

² http://waterberichtgeving.rws.nl/nl/water-en-weer_dataleveringen_ophalen-opgetreden-data.htm

³ http://waterberichtgeving.rws.nl/nl/water-en-weer_dataleveringen_ophalen-opgetreden-data.htm

⁴ <http://opendap.deltares.nl/thredds/catalog/opendap/knmi/potwind/catalog.html>

⁵ http://www.knmi.nl/samenw/hydra/cgi-bin/meta_data.cgi

Wind_v, wind_dir	VvdR	Potwind, KNMI-website ⁵	1997-2005

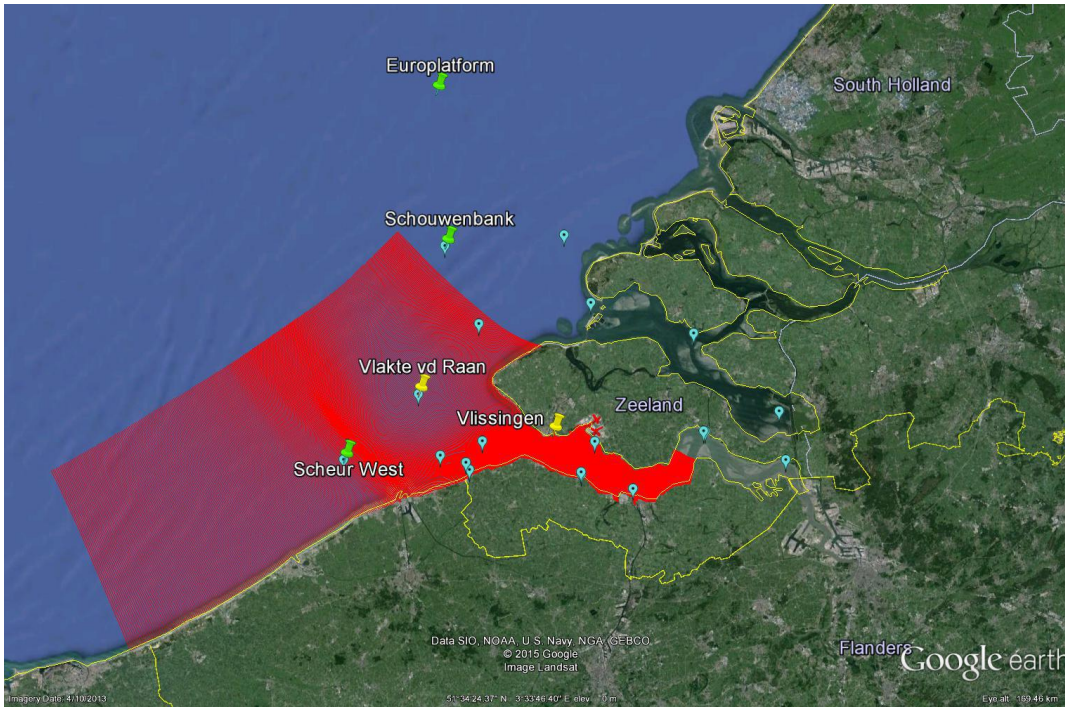


Figure A.1 Overzicht meetlocaties golf- en winddata. Alle beschikbare HMCZ-locaties voor golfdata (linksboven), en winddata (rechtsboven). Belangrijkste locaties ten opzichte van modelgrid (onder).

A.2.2 Wave data

The wave data, measured at station Schouwenbank, is shown in Figure A.2 and Figure A.3 . In total roughly 7 years of data is available for the analysis.

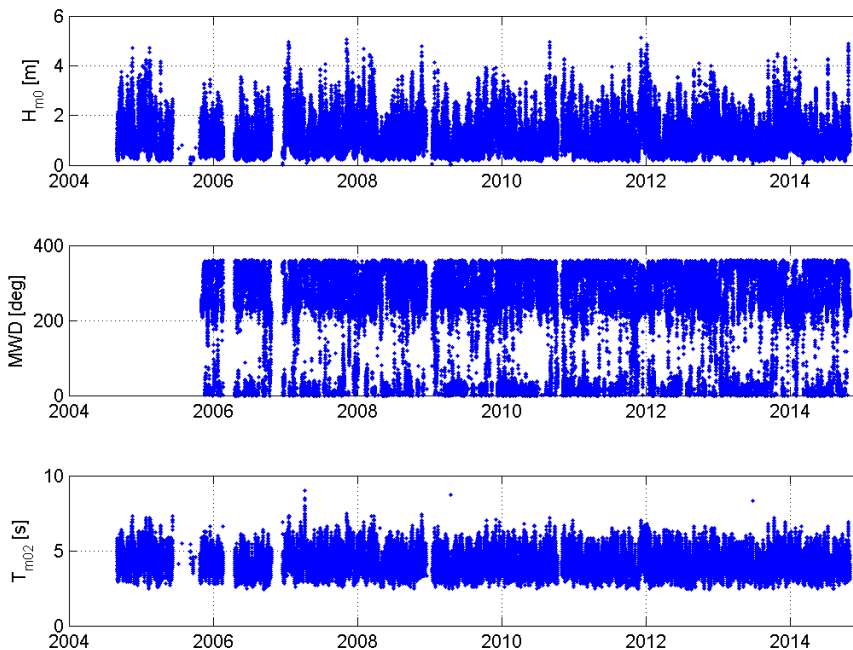


Figure A.2 Golfgegevens voor Schouwenbank (2004-2014)

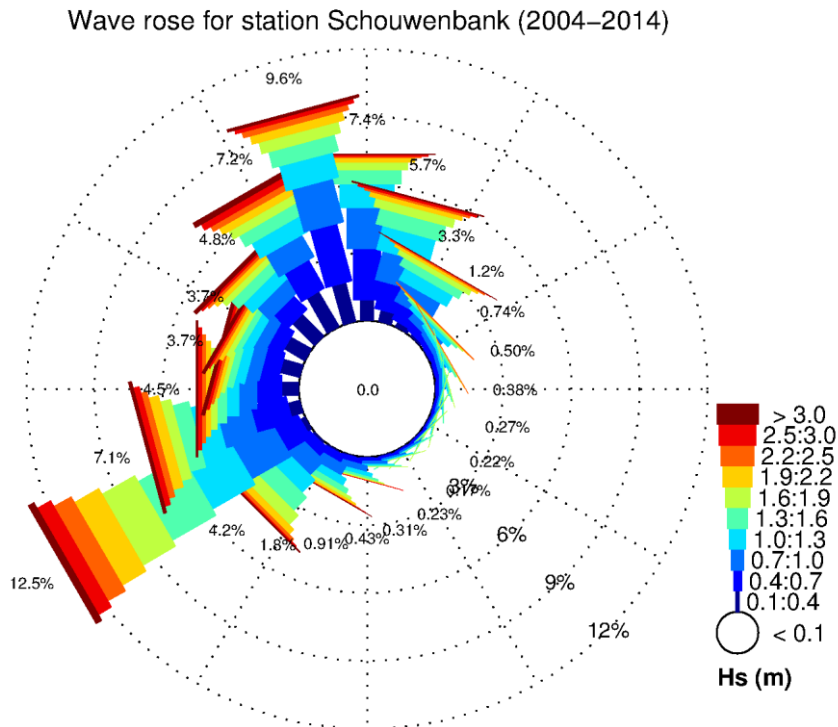


Figure A.3 Golfroos op basis van golfgegevens Schouwenbank (2004-2014)

A.2.3 Wind data

The available wind data is shown in Figure A.5 for two stations: Vlakte van de Raan and Vlissingen. The locations of both stations are shown in Figure A.1. For both stations, wind data is available for the period of wave measurements. The data at Vlakte van de Raan is chosen to be used further due to its more exposed and central location. The wind data measured at that station is considered more representative for the accompanying wave conditions at Schouwenbank.

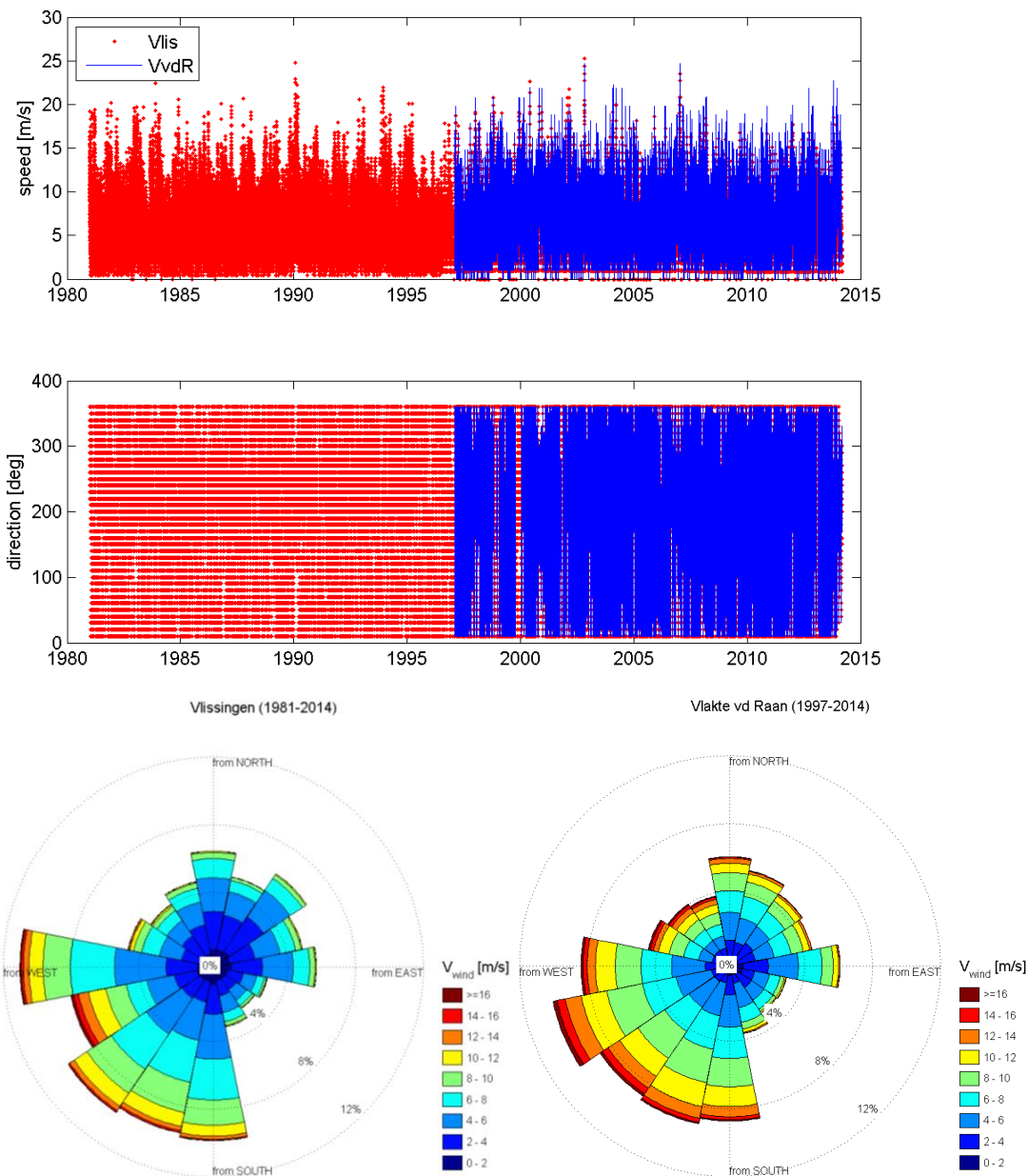


Figure A.4 Wind data for station Vlissingen and Vlakte v.d. Raan (source: KNMI, <http://opendap.deltares.nl/thredds/catalog/opendap/knmi/potwind/catalog.html>).

A.3 Wave climate schematization

There are several methods of schematizing a wave climate. Some, earlier studies make use of the OPTI-method (e.g. Van Rijn, 2012; Damen, 2014), which is a routine that automatically determines a set of optimal settings based on a given wave record. However, a disadvantage of this method is that it may result in wave conditions that are very different compared to the measured values, yet give a similar result in morphodynamic impact or net transports. While these conditions would still give an accurate representation of the results computed with the full wave climate, it is difficult to communicate the choice for such conditions with other parties.

Therefore, we use a more practical method here, in which the wave climate is first schematized in a large number of bins, and these bins are later grouped. The grouping is

based on the cumulative morphological impact, and the final resulting set of wave conditions is compared to the results for a simulation with the full wave climate. In order to keep run times practical, we choose to run all conditions for a representative tidal cycle or morphological tide.

A.3.1 Morphological tide

To come up with a representative tidal cycle, we ran a single domain version of the NeVla model (Van der Werf et al., 2015) for a full spring neap cycle (09-03-2006 00:00 until 23-03-2006 10:30). Then the mean total transports were computed for the full period, as well as the mean transports per individual tide. The results for each individual tide were compared to the results for the full period (see Figure A.5). Focussing on the mouth of the estuary, the period 13-03-2006 17:30 until 14-03-2006 05:00 turned out to be the most representative tidal cycle for a full spring neap cycle.

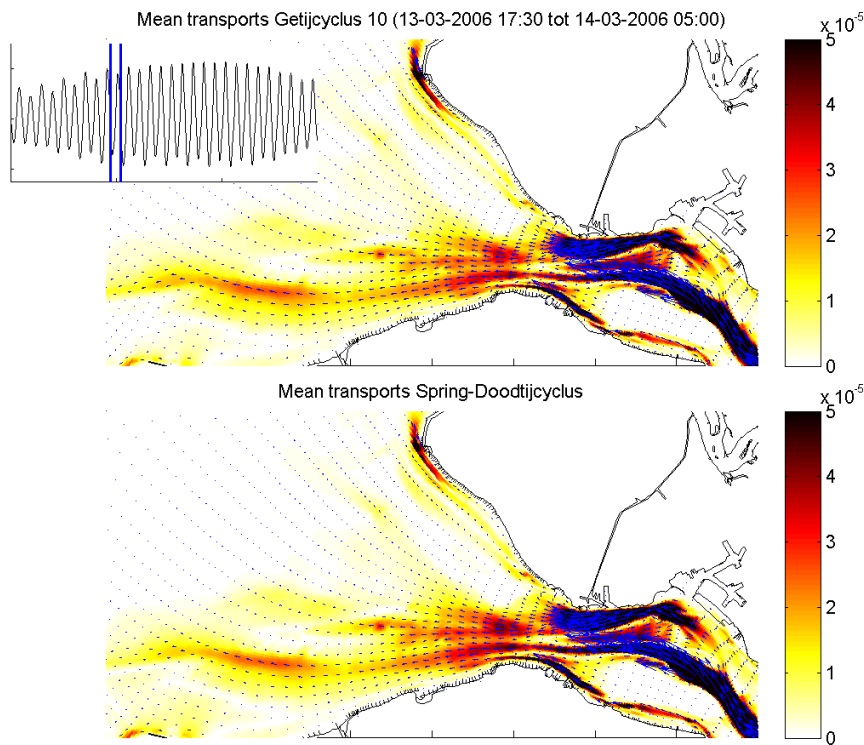


Figure A.5 Best result for mean total transports for morphological tide (13-03-2006 17:30 until 14-03-2006 05:00, top panel) compared to the mean total transports associated with a full spring neap cycle (bottom).

A.3.2 Derivation of wave conditions

First all data points are categorized based on the wave height and mean wave direction. For the wave height a resolution of $dH = 0.1$ m is used, and for the wave direction $d\Theta = 1$ deg. This results in $\sim 22,000$ (61×361) different wave conditions, however, as can be seen in Figure A.6 in most of the bins only a few or even no data points are located.

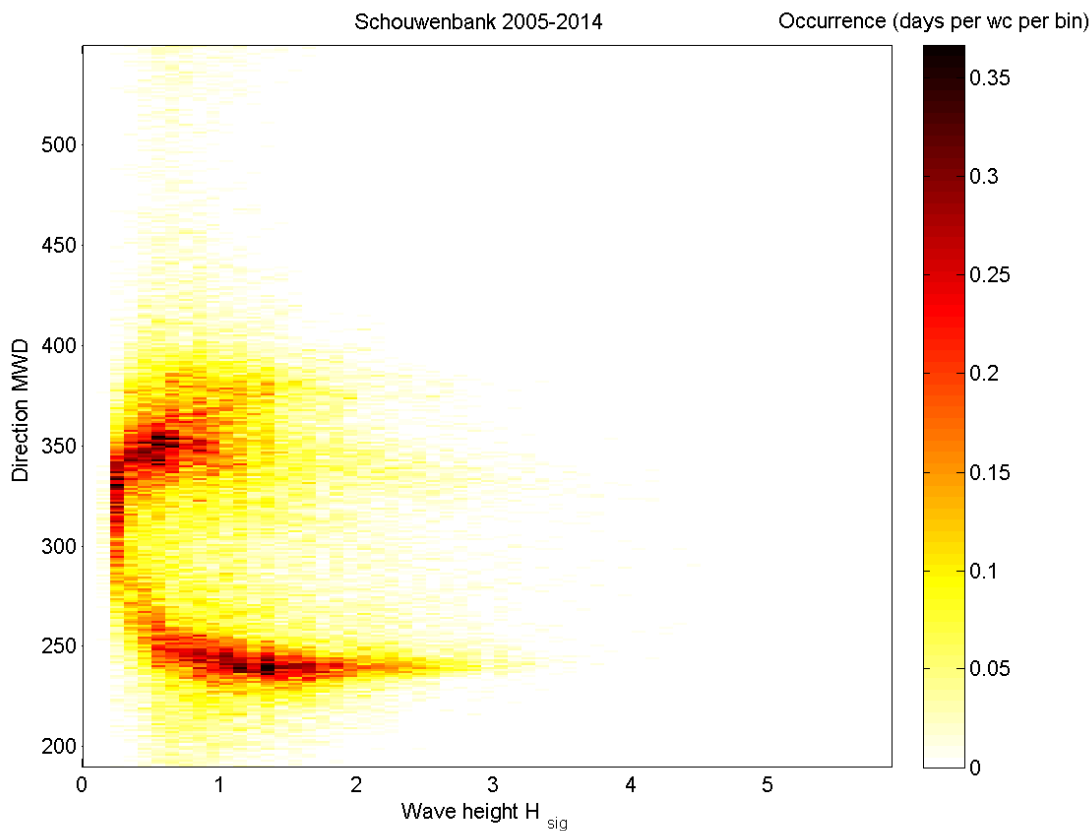


Figure A.6 Wave climate schematization for wave data at Schouwenbank. The color represents the occurrence of each individual wave condition.

In the sections below the high resolution schematization is reduced to respectively 1, 2, 4 and 6 wave conditions. The schematization is chosen such that the potential morphological impact for each condition of the derived morphological wave climate is more or less equal. To determine the morphological impact of a wave condition, we assume that $H^{2.5}$ is representative for sediment transport. This parameter is commonly used in wave climate schematizations and is based on the relation between longshore sediment transport and wave height in the CERC-formula.

The schematizations are validated by running a number of morphological simulations (equal to the number of wave conditions) in which the morphological tide is used to get a representative tidal effect. The mean total transport is computed in a simulation for each individual wave condition over the full tidal cycle. The weighted mean transports are then obtained by adding the results per wave condition, multiplied with the probability of occurrence.

In the following sections, the definition and validation per wave condition are discussed. The resulting wave conditions are also available in a mat-file⁶.

⁶ p:\1209395-schelde\golfklimaat\wclimate\

A.3.2.1 Wave climate representation in 1 condition

To get one wave condition representative for the entire wave climate, the weighted average wave height and wave direction are computed. The results are shown below.

Table A.2 Overview of conditions for wave climate schematization in 1 condition

Condition #	Hm0 [m]	Tp [s]	MWD [deg]	Uwind [m/s]	Udir [deg]	P [-]
1	1.41	6.5	292	5.5	261	1

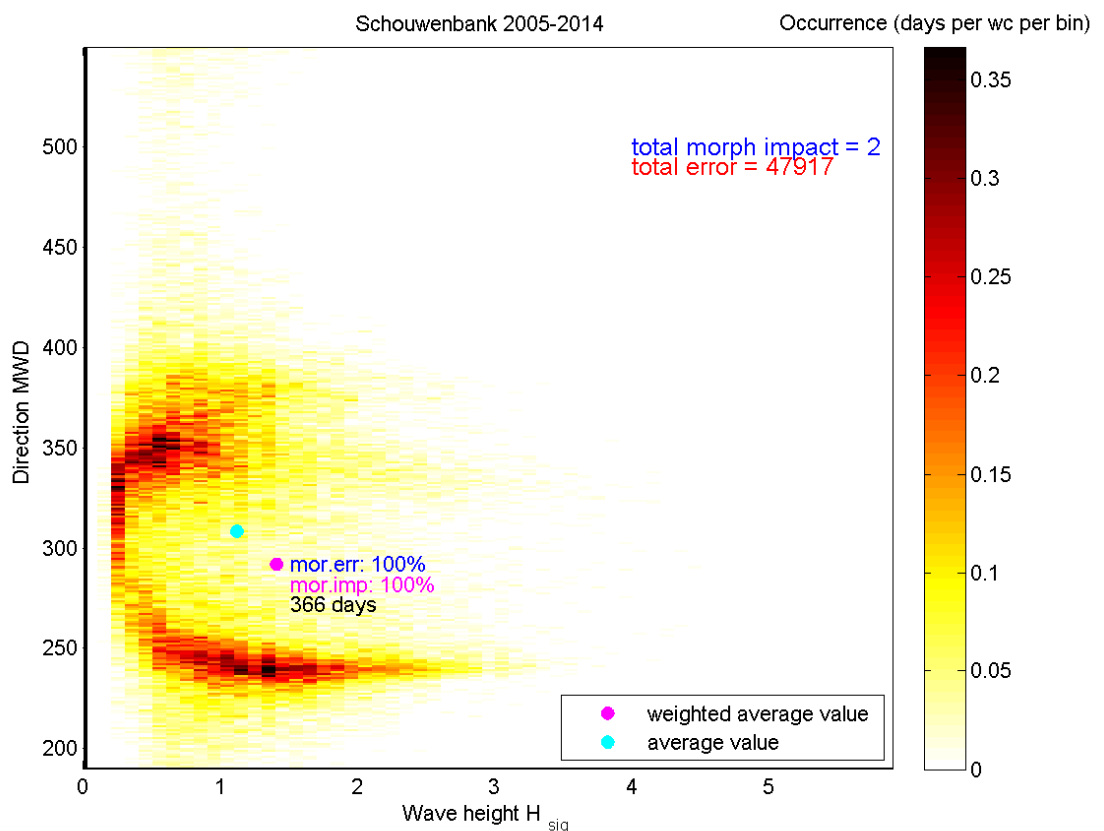


Figure A.7 Schematization of wave climate in one wave condition.

A.3.2.2 Wave climate representation in 2 conditions

To get two wave condition representative for the entire wave climate, the weighted average wave height and wave direction are computed for two representative wave bins. The results are shown below.

Table A.3 Overview of conditions for wave climate schematization in 2 conditions

Condition #	Hm0 [m]	Tp [s]	MWD [deg]	Uwind [m/s]	Udir [deg]	P [-]
1	1.5324	6.2998	243.3106	10.7874	228.2832	0.4069
2	1.3102	6.7307	339.3740	6.2564	334.4685	0.5931

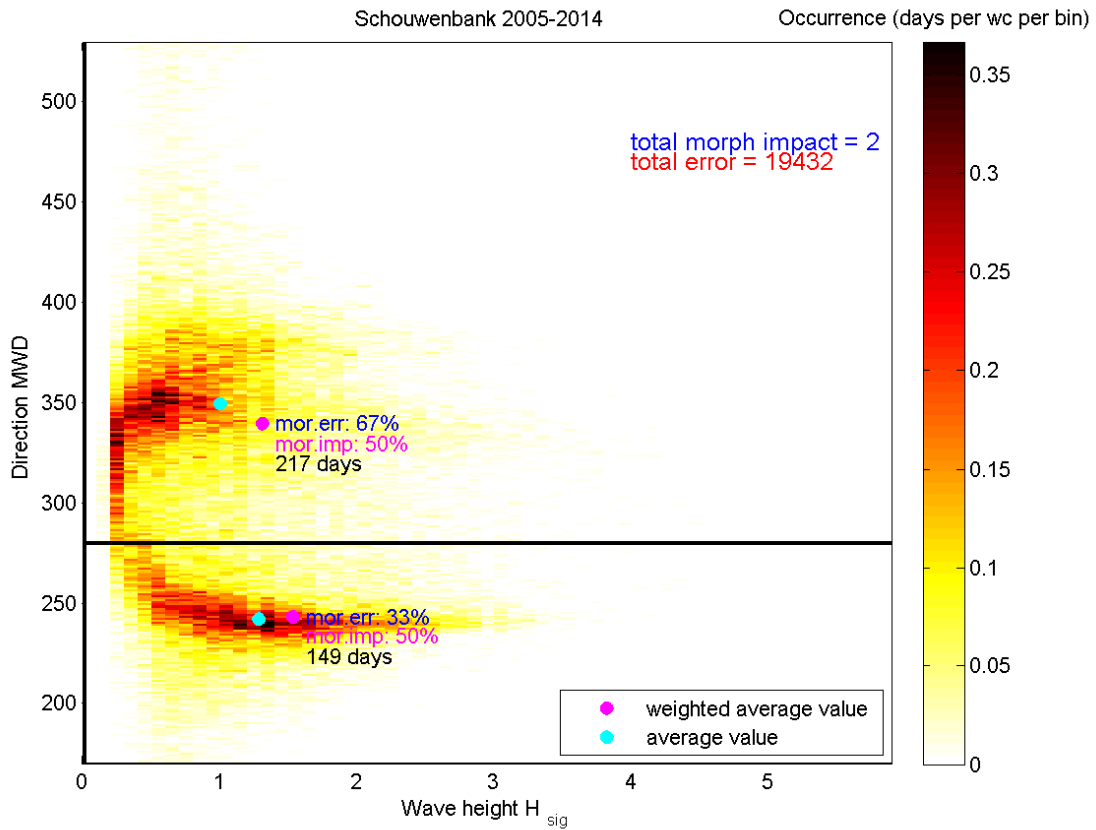


Figure A.8 Schematization of wave climate in two wave conditions.

A.3.2.3 Wave climate representation in 4 conditions

To get four wave condition representative for the entire wave climate, the weighted average wave height and wave direction are computed for four representative wave bins. The results are shown below.

Table A.4 Overview of conditions for wave climate schematization in 4 conditions

Condition #	Hm0 [m]	Tp [s]	MWD [deg]	Uwind [m/s]	Udir [deg]	P [-]
1	1.1889	5.5664	242.7767	8.3041	220.2054	0.3637
2	1.0127	5.8931	355.8915	3.3654	8.5072	0.5226
3	2.5538	6.9599	248.9128	12.6748	236.9848	0.0666
4	2.6797	7.5162	333.3055	9.5574	331.1870	0.0471

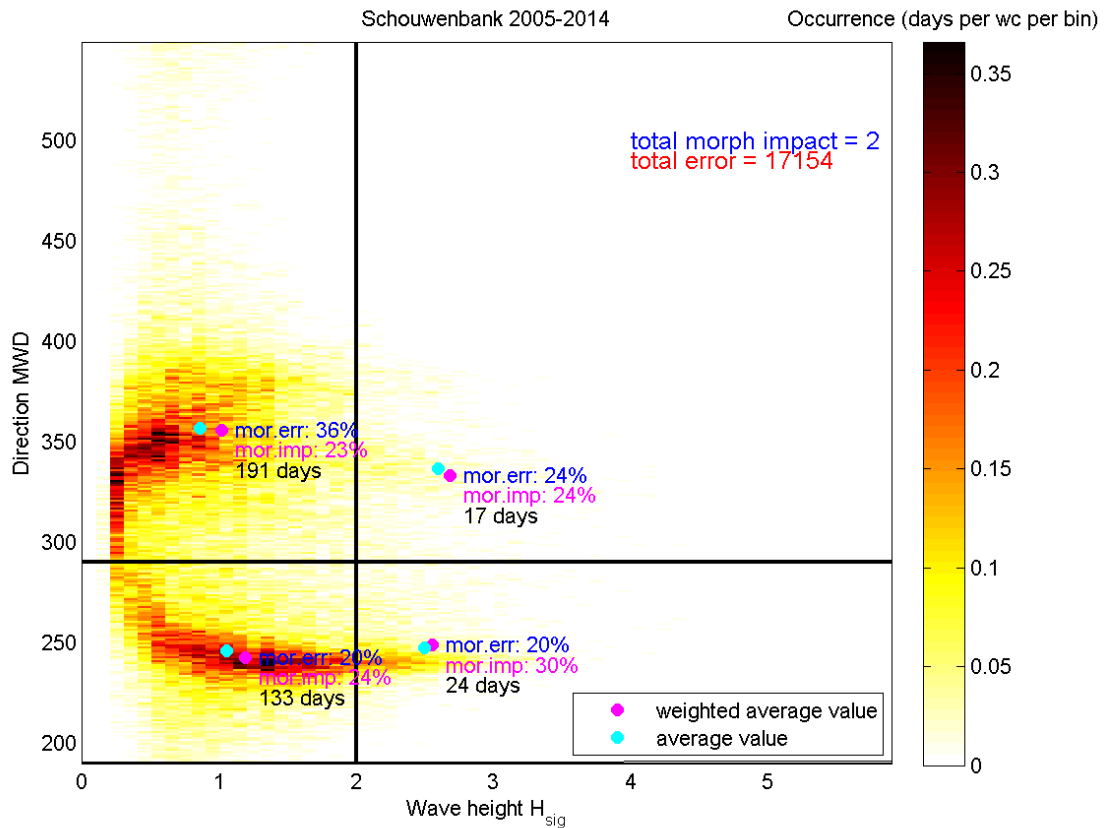


Figure A.9 chematization of wave climate in four wave conditions.

A.3.2.4 Wave climate representation in 6 conditions

To get six wave condition representative for the entire wave climate, the weighted average wave height and wave direction are computed for six representative wave bins. The results are shown below. In the figure 9 bins are shown, however for three of the wave conditions the wave direction is in offshore direction, while the morphological impact of these conditions is very low. These conditions are therefore neglected, resulting in 6 wave conditions.

Table A.5 Overview of conditions for wave climate schematization in 6 conditions

Condition #	Hm0 [m]	Tp [s]	MWD [deg]	Uwind [m/s]	Udir [deg]	P [-]
1	0.9741	5.1856	243.4418	6.9650	217.7407	0.2902
2	0.8628	5.6710	351.3306	2.8429	14.1988	0.4309
3	1.9283	6.2176	243.8416	10.4068	225.9840	0.1141
4	1.9105	6.5993	343.4355	6.0363	348.4688	0.0804
5	2.9685	7.3126	251.5470	13.8893	241.7145	0.0259
6	3.1155	7.8543	329.7482	11.0148	327.2485	0.0212

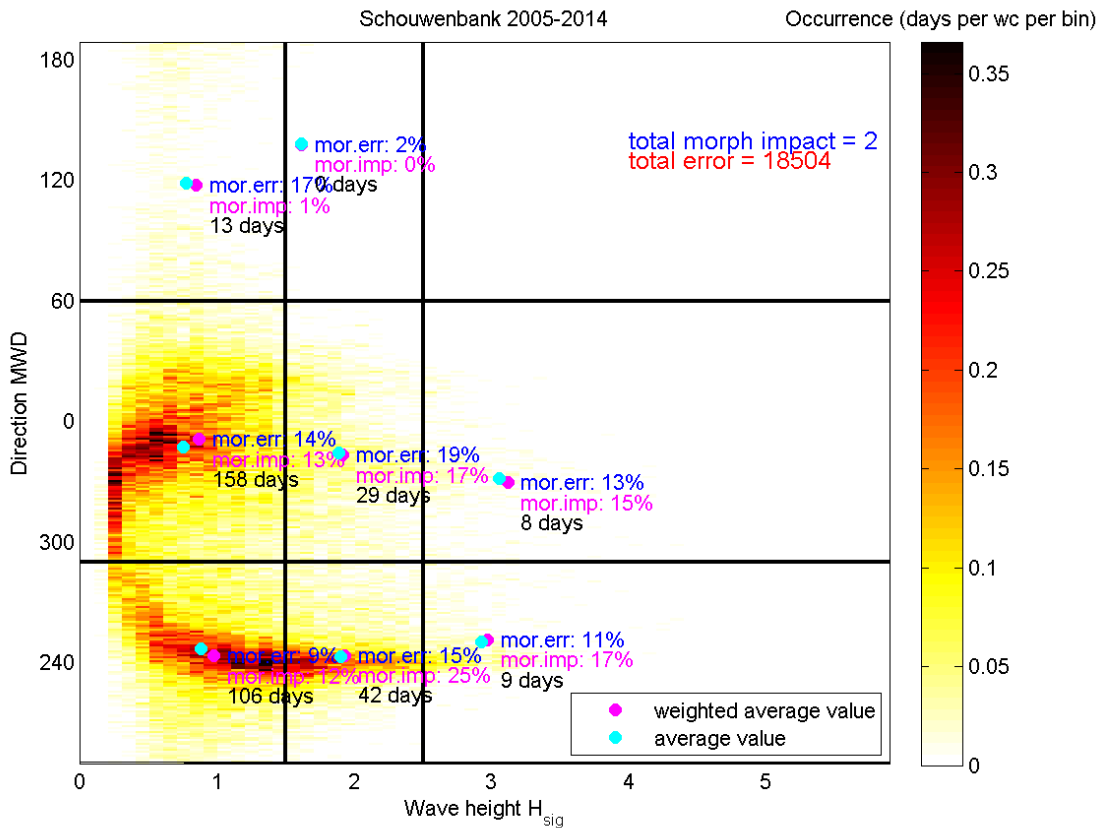


Figure A.10 Schematization of wave climate in six wave conditions.

A.3.3 Validation of wave schematizations⁷

For every combination of wave conditions, simulations over one morphological tide were carried out. For instance, for the schematization with 4 wave conditions, 4 simulations are carried out with those conditions. Then the results are summed by weight (probability of occurrence) to get an approximation of the computed mean transports using a certain schematization.

The results are compared to a similar method for the full climate. Ideally we would use all 61x361 wave conditions specified above, but this would result in an unworkable amount of simulations. The wave climate is therefore re-schematized in bins with $dH = 0.5$ m and $d\theta = 15$ degrees, resulting in a total of 288 wave conditions. For each of these wave conditions the potential morphological impact was determined (assuming $H^{2.5}$), and the conditions were selected for which the relative morphological impact was higher than 0.5%. This resulted in 66 wave conditions, which is considered accurate enough to represent the full wave climate. So, for all 66 wave conditions a morphological simulation over one morphological tide was carried out, and the results were summed by weight. The results are shown on the next pages per schematized climate.

⁷ Scripts: p:\1209395-schelde\golflimaat\verify\

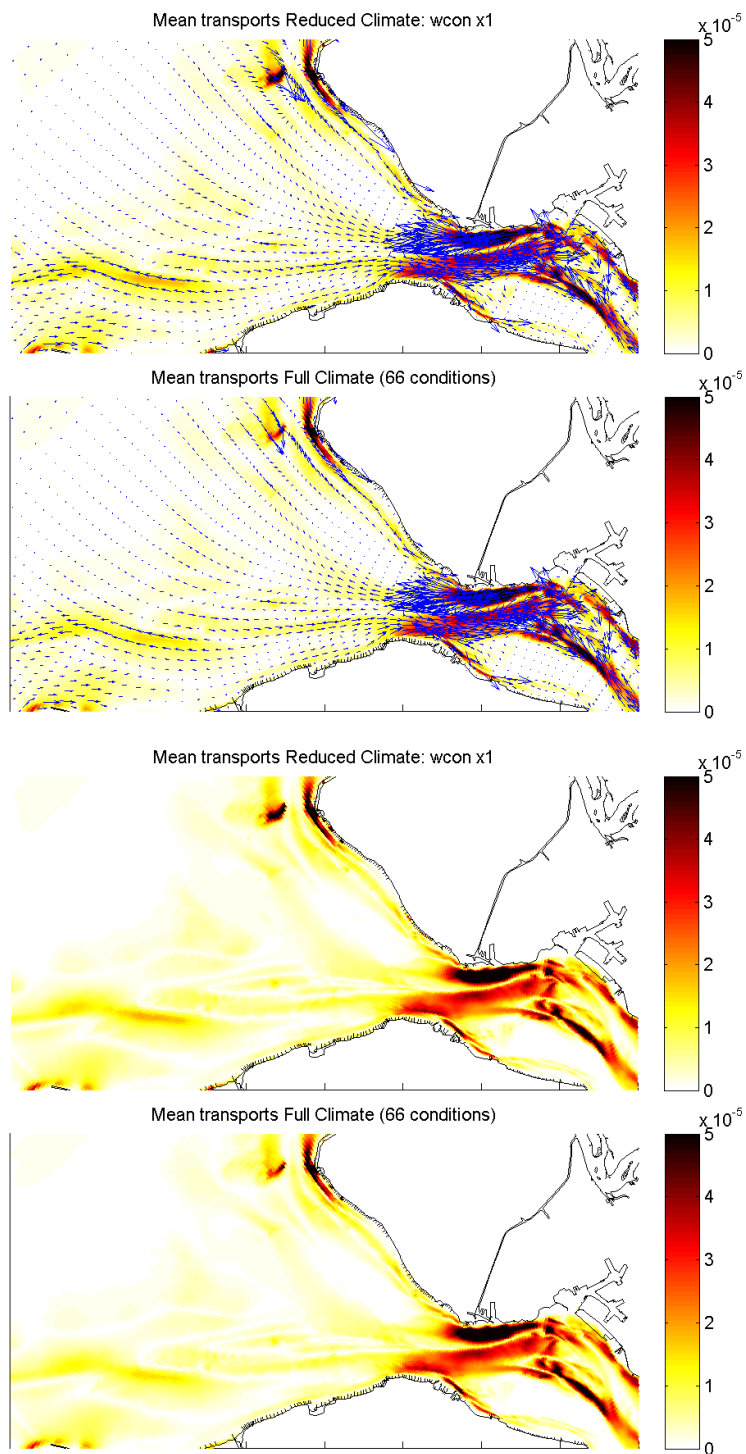


Figure A.11 Results for one wave condition (top) vs. 66 wave conditions (bottom).

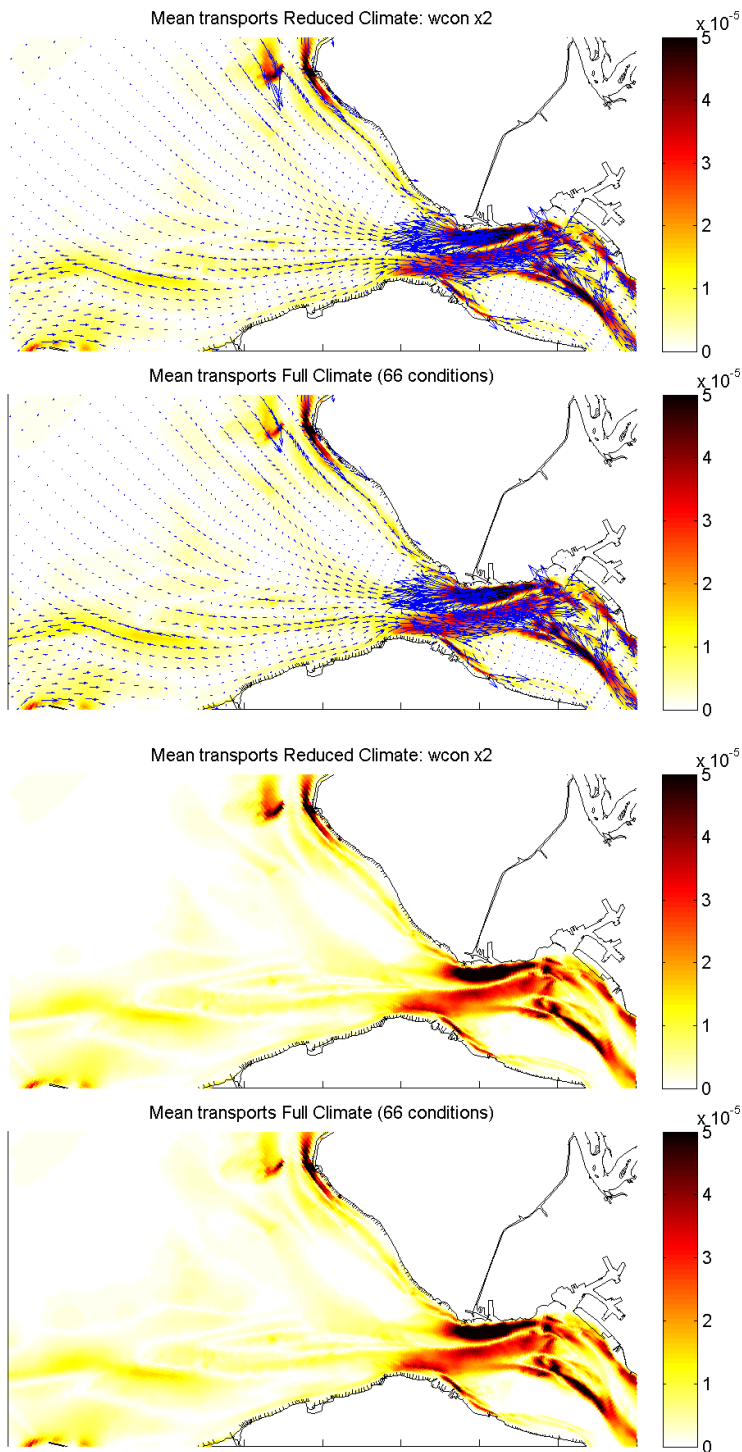


Figure A.12 Results for two wave conditions (top) vs. 66 wave conditions (bottom).

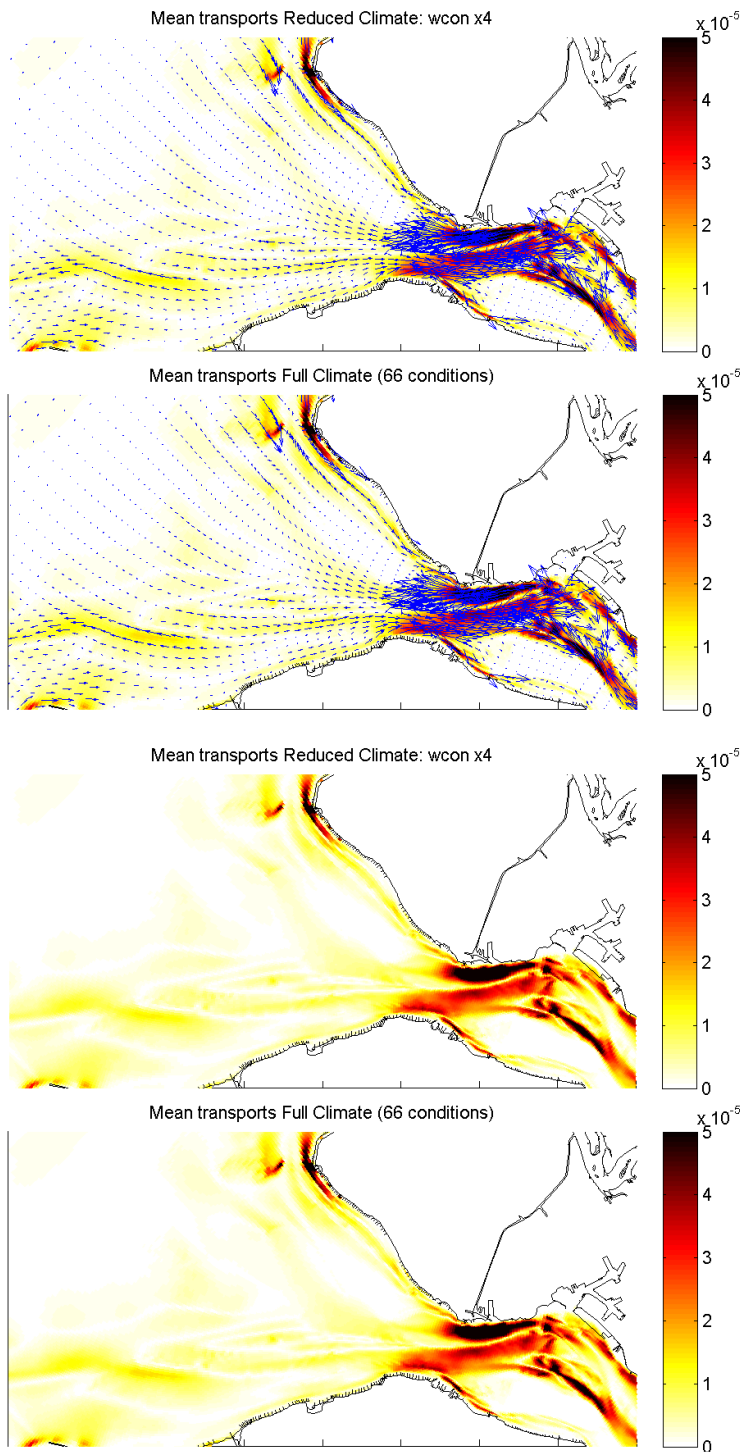


Figure A.13 Results for four wave conditions (top) vs. 66 wave conditions (bottom).

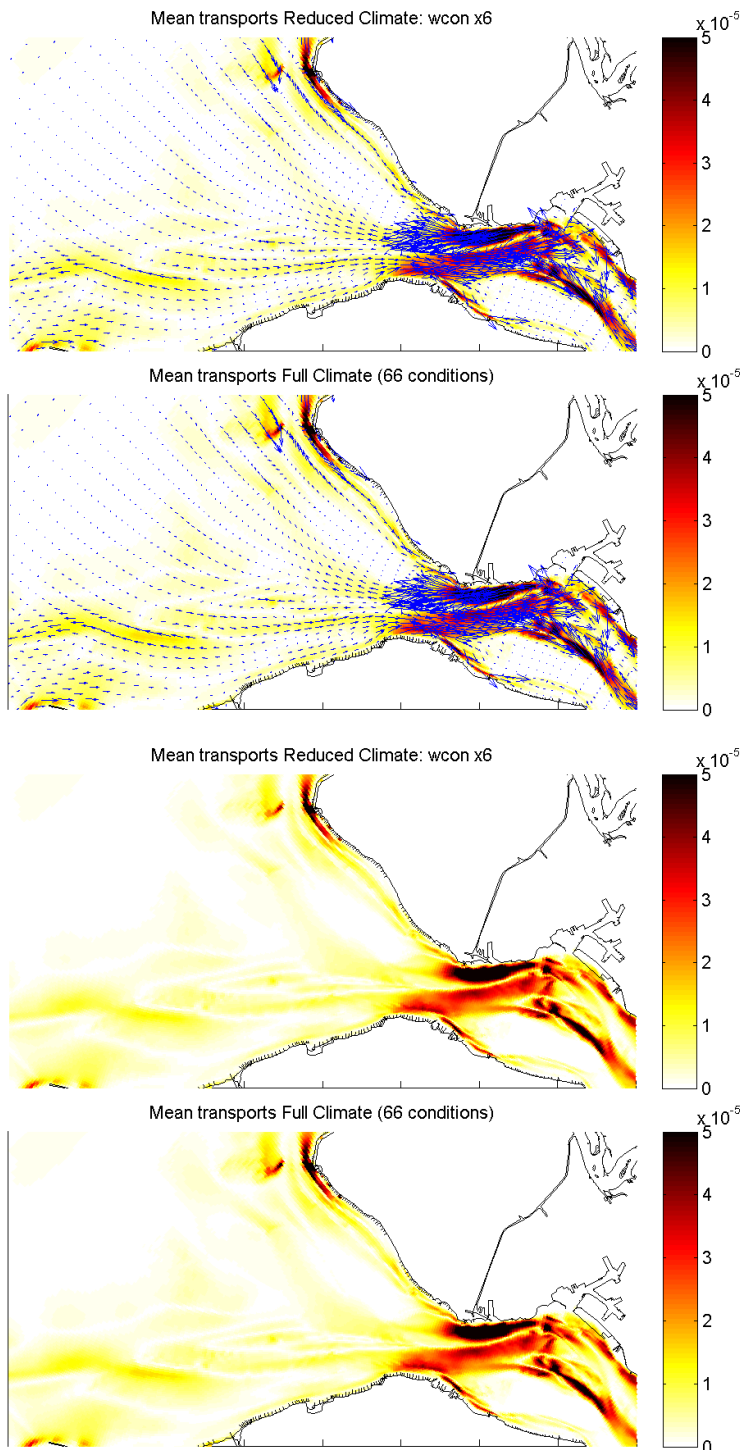


Figure A.14 Results for six wave conditions (top) vs. 66 wave conditions (bottom).

When making a qualitative comparison between the mean total transports associated with the 'full' climate and with the schematized climates, it can be seen that the results for all schematizations are rather similar. Especially for four wave conditions and six conditions the results look very much alike.

A.4 References

Damen, John. "Coastal erosion processes in tidal channel Oostgat." (2014).

Van Rijn, B. W. F. *Influence of wave climate schematisation on the simulated morphological development of the Westerschelde entrance*. Diss. TU Delft, Delft University of Technology, 2012

B BSS definition

In order to assess the skill of morphodynamic models Sutherland et al. (2004) suggest the use of the Brier Skill Score (BSS). For the current study the BSS is defined as follows:

$$BSS = 1 - \frac{\langle (\Delta vol_{mod} - \Delta vol_{meas})^2 \rangle}{\langle \Delta vol_{meas}^2 \rangle} \quad (2.1)$$

in which

Δvol volumetric change compared to the initial bed, (m^3)
 mod modeled quantity,
 $meas$ measured quantity

and the $\langle \rangle$ denote an arithmetic mean (a spatial average in this case).

A BSS of 1 is a perfect model, whereas lower values indicate poorer model performance. Sutherland et al. (2004) note that the BSS is unbounded at the lower limit and that the BSS can be extremely sensitive to small changes when the denominator is low.

The origin of a particular BSS value may be attributed to an amplitude error, a phase error, or a deviation from the average value. In the first case an error is made in the 'height' of a particular morphological feature, in the second case the BSS is degraded by a shift in location of the morphologic feature, whereas in the latter case the error originates from a deviating mean bed level. In order to assess these errors separately, Murphy and Epstein (1989) suggest to decompose the BSS as follows:

$$BSS = \frac{\alpha - \beta - \gamma + \varepsilon}{1 + \varepsilon} \quad (2.2)$$

In which

$$\begin{aligned} \alpha &= r_{X'Y'}^2 \\ \beta &= \left(r_{X'Y'} - \frac{\sigma_{Y'}}{\sigma_{X'}} \right)^2 \\ \gamma &= \left(\frac{\langle Y' \rangle - \langle X' \rangle}{\sigma_{X'}} \right)^2 \\ \varepsilon &= \left(\frac{\langle X' \rangle}{\sigma_{X'}} \right)^2 \end{aligned} \quad (2.3)$$

And

r correlation coefficient
 σ standard deviation
 X' Δvol_{meas} , m^3
 Y' Δvol_{mod} , m^3

Following Sutherland et al. (2004) α is a measure of phase error. Perfect modeling of the phase gives $\alpha = 1$. β is a measure of the phase and amplitude error. Perfect modeling of phase and amplitude gives $\beta = 0$. γ is a measure of the mean error when the predicted average bed level is different from the measured, and perfect modeling of the mean gives $\gamma=0$. 'ε' is a normalization term, which is only affected by measured changes from the baseline prediction.

In order to account for the effect of measurement errors Van Rijn et al. (2003) suggest the following extended BSS:

$$BSS_{vR} = 1 - \frac{\langle (|\Delta vol_{mod} - \Delta vol_{meas}| - \delta)^2 \rangle}{\langle \Delta vol_{meas}^2 \rangle} \quad (2.4)$$

in which δ (m³) is the volumetric measurement error and in which $|\Delta vol_{mod} - \Delta vol_{meas}| - \delta$ is set to zero if $|\Delta vol_{mod} - \Delta vol_{meas}| < \delta$. Van Rijn et al. (2003) proposed a classification of BSS and BSS_{vR} values as presented in Table 7.1.

	BSS	BSS _{vR}
Excellent	0.5-1.0	0.8-1.0
Good	0.2-0.5	0.6-0.8
Reasonable	0.1-0.2	0.3-0.6
Poor	0.0-0.1	0.0-0.3
Bad	< 0.0	< 0.0

Table 7.1 BSS classification

C Detailed model results

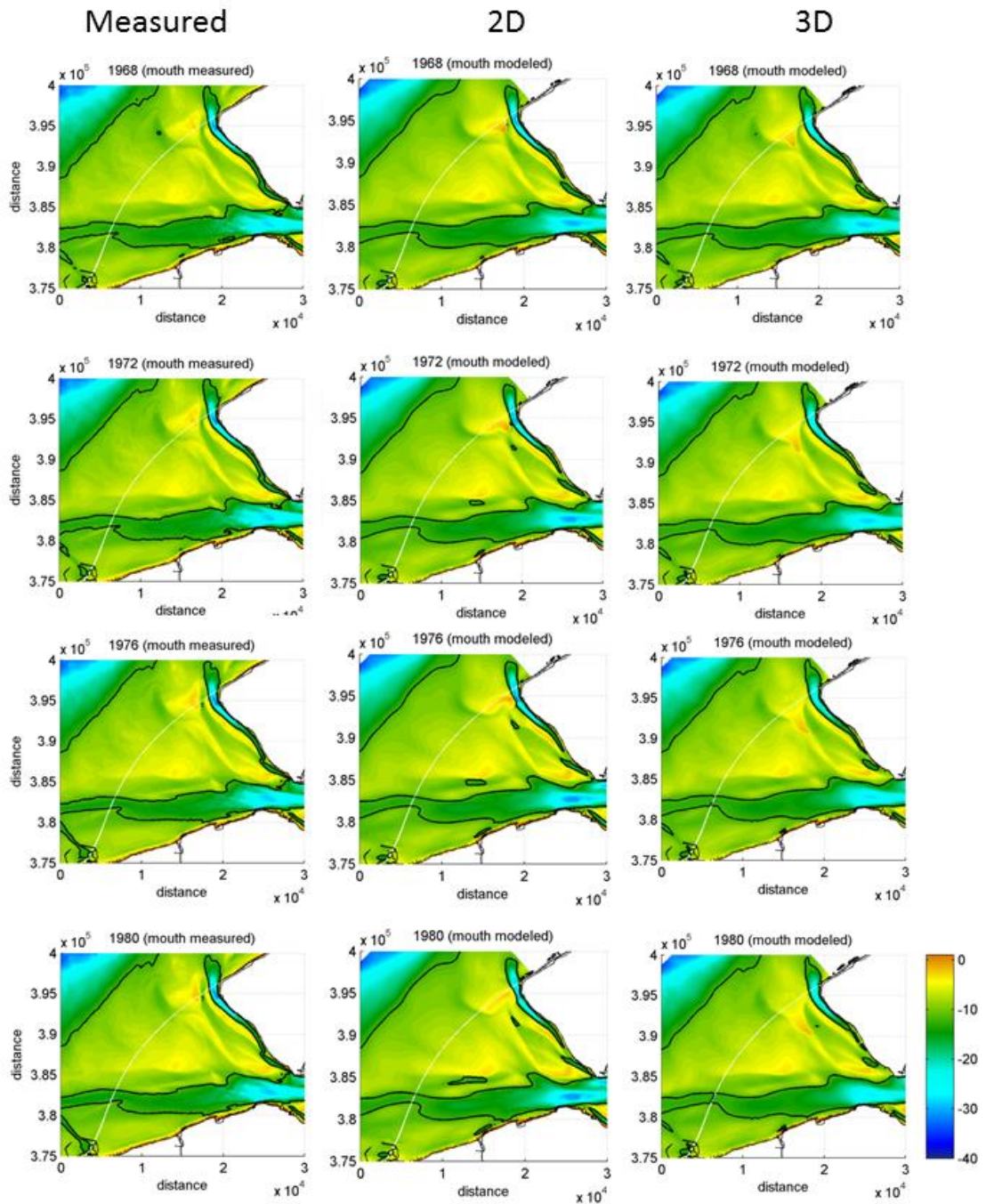


Figure C.1 Bathymetric development (measured and modelled) for years 1968-1980

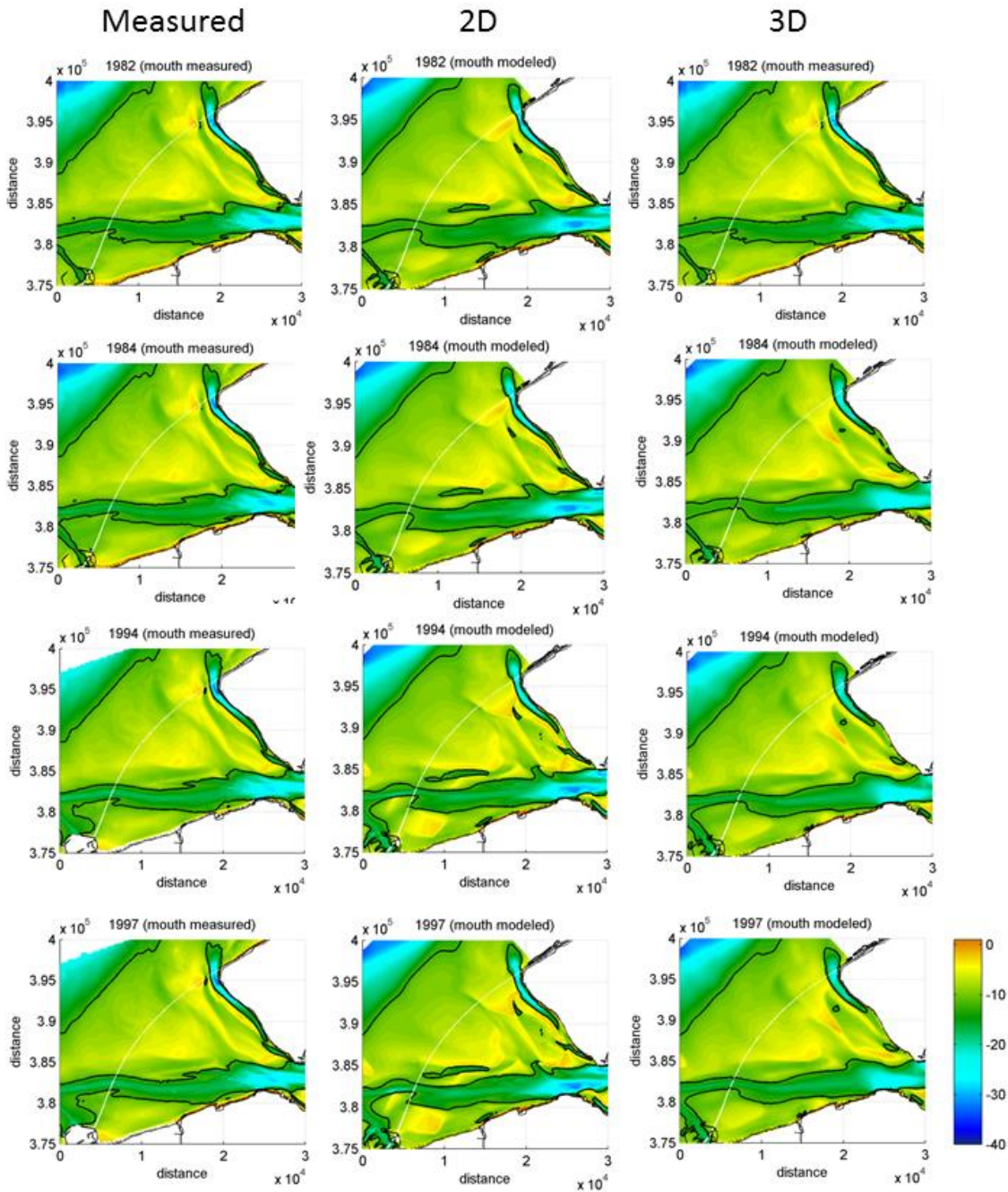


Figure C.2 Bathymetric development (measured and modelled) for years 1984-1997

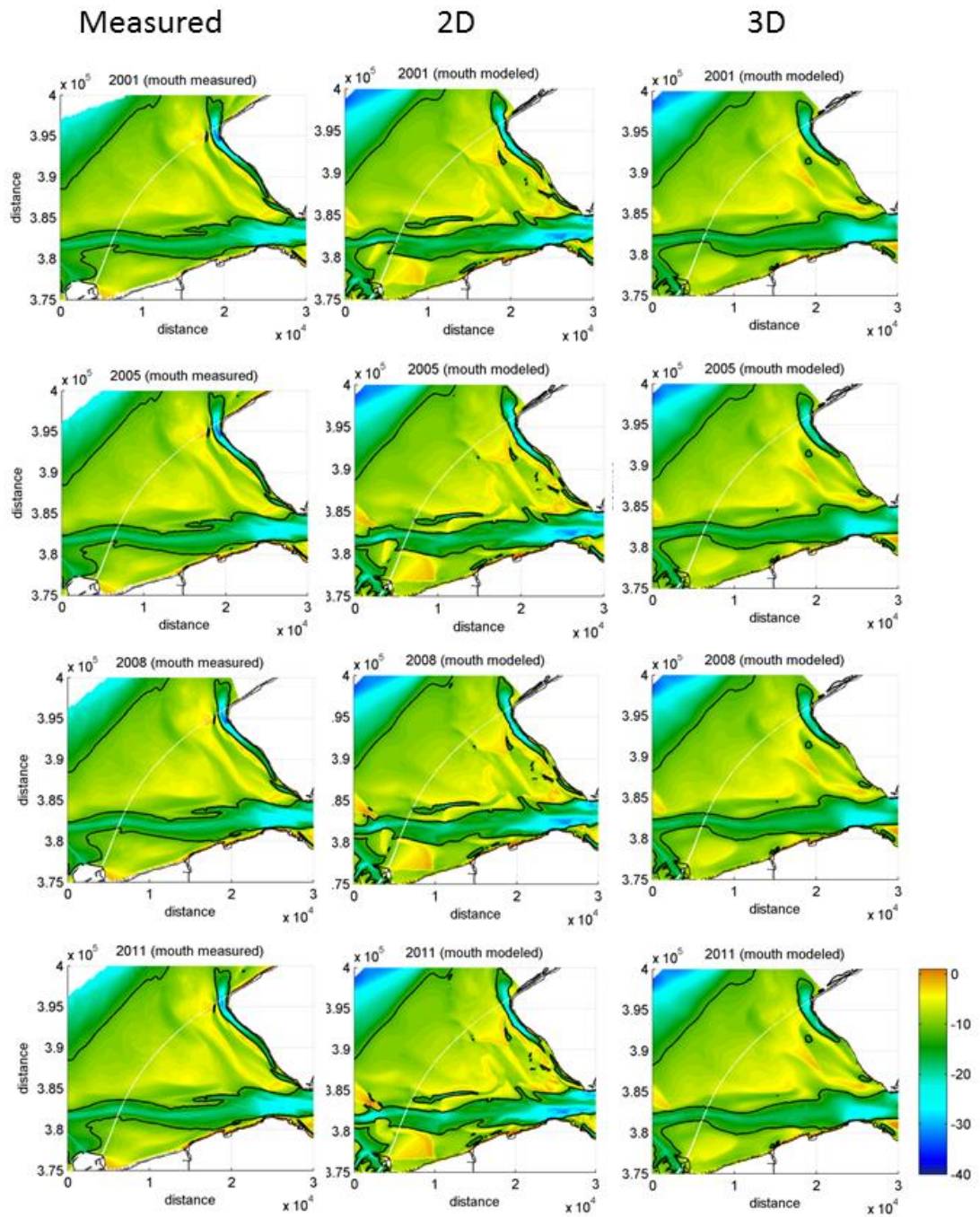


Figure C.3 Bathymetric development (measured and modelled) for years 2001-2011

D Detailed model results of dredging activities

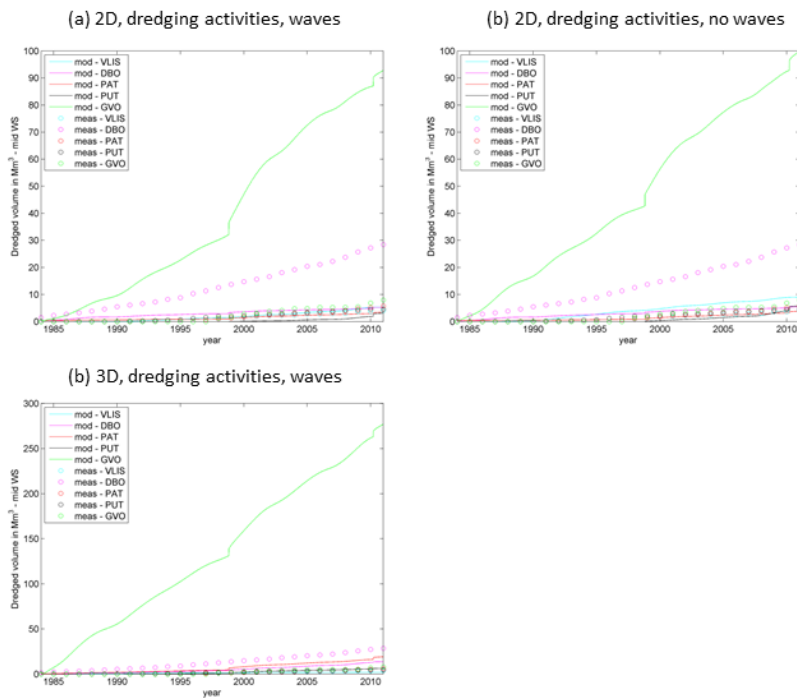


Figure D.1 Modelled and measured dredging volumes for mid -Westerschelde region

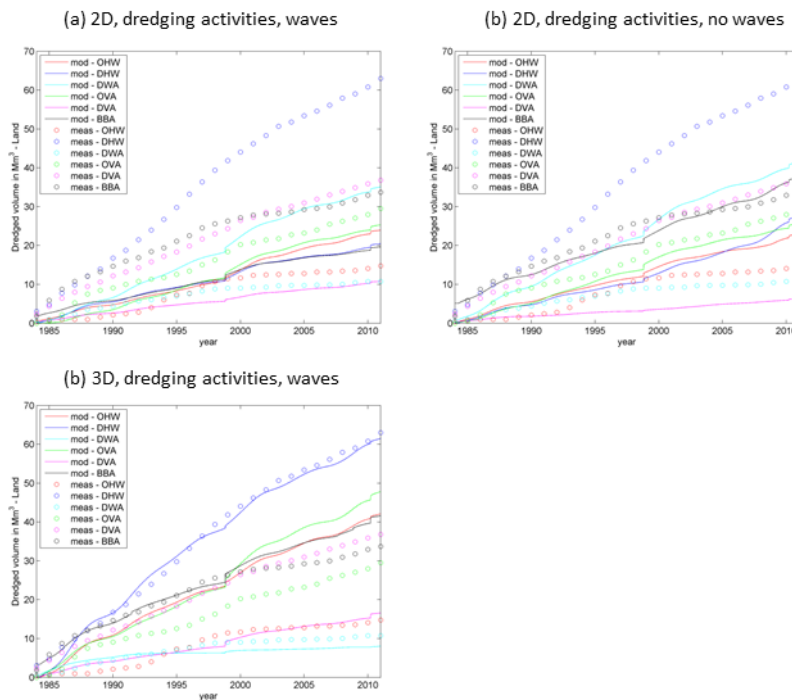


Figure D.2 Modelled and measured dredging volumes for eastern Westerschelde region